Centro de Investigación y de Estudios Avanzados
del
Instituto Politécnico Nacional

DEPARTAMENTO DE FÍSICA

Mecanismo de un lazo para desintegraciones doble beta sin neutrinos de hiperones

Tesis que presenta

Diego Portillo Sánchez

para obtener el Grado de

Maestro en Ciencias

en la Especialidad de

Física

Directores de tesis: **Dr. Gabriel López Castro**
Dr. Gerardo Hernández Tomé

Ciudad de México Septiembre, 2021

CENTRO DE INVESTIGACION Y DE ESTUDIOS AVANZADOS DEL INSTITUTO POLITECNICO NACIONAL

PHYSICS DEPARTMENT

"One loop mechanism for neutrinoless double beta decays of hyperons"

Thesis submitted by

Diego Portillo Sánchez

In order to obtain the

Master of Science

degree, speciality in

Physics

Supervisors: **Dr. Gabriel López Castro**
Dr. Gerardo Hernández Tomé

Mexico City September, 2021.

CENTRO DE INVESTIGACIÓN Y ESTUDIOS AVANZADOS DEL IPN

DEPARTAMENTO DE FÍSICA

A THESIS SUBMITTED FOR THE DEGREE OF
MASTER OF SCIENCE:

ONE LOOP MECHANISM FOR NEUTRINOLESS DOUBLE BETA DECAYS OF HYPERONS

Diego Portillo Sánchez.

Advisors:
Dr. Gabriel López Castro
Dr. Gerardo Hernández Tomé

Dedicated to my family

Acknowledgements

I would like to express my gratitude to my advisors, Dr. Gerardo Hernández Tomé and Dr. Gabriel López Castro for all the help and support that gave me throughout the realization of this project. I would also like to thank Dr. Pablo Roig Garcés and Dr. Ivan Heredia de la Cruz for their helpful comments as well as Conacyt for the financial support. I wish to extend my thanks to my friends and colleagues whose company made these two years a great experience. Finally, i want to express my sincere thanks to my siblings Jazael, Lisset, Jesús and Vanesa for all their unconditional support, as well as to my parents Araceli and Adrián whose love and affection drive me every day.

Resumen

Es bien sabido que cualquier observación de violación de número leptónico tendría implicaciones en la comprensión del sector de neutrinos y física más allá del modelo estándar. En esta tesis estudiamos los decaimientos doble-beta sin neutrinos de hiperones originados a través de un modelo de lazo que involucra bariones y neutrinos de Majorana como estados intermedios. Proporcionamos una estimación confiable para los valores máximos de todos los canales posibles. A diferencia de trabajos previos, nuestros resultados toman en cuenta los efectos de la interacción fuerte en el cálculo del lazo asumiendo una estructura razonable para los factores de forma vectorial y axial de los estados hadrónicos intermedios conduciendo a un resultado libre de divergencias ultravioletas. Exploramos dos escenarios interesantes compatibles con los límites actuales del sector de neutrinos, a decir, las contribuciones de tres neutrinos ligeros de Majorana, así como el caso de neutrinos pesados con masas alrededor de unos pocos TeV predichos por los llamados modelos de *seesaw de baja energía*.

Abstract

It is well know that any observation of lepton number violation would have implications on the comprehension of the neutrino sector and physics beyond the standard model. This thesis studies the neutrinoless double-beta decays of hyperons triggered by an effective one-loop model mechanism involving baryons and Majorana neutrinos as intermediate states. We provide a reliable estimate of the maximum branching fractions for all the possible channels. Unlike previous works, our results take into account the effects of the strong interaction in the loop computation assuming a reasonable structure for the vector and axial form factors of the hadronic intermediate states leading to a result free of ultraviolet divergences. We explore two interesting scenarios compatible with the current limits of the neutrino sector, namely, the contributions of three light Majorana neutrinos, and the case of heavy Majorana masses around few TeV predicted by the so-called *low-scale seesaw* models.

Contents

Introduction

On July 4th 2012, the experiments Compact Muon Solenoid (CMS) and A Toroidal LHC ApparatuS (ATLAS) at the European Organization for Nuclear Research (CERN) announced the observation of a new particle in the mass region around 125 GeV consistent with the so-called Higgs boson [1,2]. This discovery represents one of the biggest milestones in the history of science contributing to our understanding of the mechanism responsible for giving mass to the subatomic particles, and completes the experimental evidence of all the elementary particles predicted by the electroweak standard model (SM).

The SM is a quantum field theory based on the principle of gauge symmetry under the $SU(3)_c \times SU(2)_L \times U(1)_Y$ group, which describes the strong, weak, and electromagnetic interactions, respectively. The SM's predictions have been successfully tested in a large diversity of experiments. Despite its enormous success, the SM does not represent the ultimate but rather an effective theory (valid until a certain scale of energy) since it is inherently an incomplete theory with some unexplained questions: What are dark energy and dark matter?, How to explain the matter-antimatter asymmetry? Are neutrinos Dirac or Majorana particles? What is the origin of the hierarchy among the masses and mixing of fermions?

Several extensions of the SM have been proposed aiming to explain some of the above questions. These hypothetical scenarios may include new particles, new couplings, and the presence of processes that were originally forbidden or extremely suppressed. However, only the evidence of such effects will set the right road towards a more fundamental theory of the elementary particles and their interactions.

One attractive place in the search for new physics (NP) is the neutrino sector. In the original formulation of the SM proposed by Glashow, Weinberg, and Salam in 1972 [3–5] neutrinos were considered massless particles. Today we know that this minimal framework must be extended to explain the observation of neutrino oscillations [6,7], which necessarily requires non-zero masses and mixings for the observed neutrinos. Then after the discovery of

neutrino oscillations phenomenon, the nature and origin of neutrinos masses has represented one of the most intriguing questions in particle physics.

Unlike charged fermions, the right-handed components for the neutrino states required to give an electroweak mass are not protected by chirality; and these new fields can generate Majorana mass terms. If Majorana masses are present, the accidental lepton number symmetry in the original formulation of the standard model is explicitly broken by two units. Therefore, the observation of lepton number violating (LNV) transitions with $\Delta \mathrm{L} = 2$ is widely viewed as the cleanest test of the Majorana nature of neutrinos. The most extensive and sensitive laboratory to probe LNV are neutrinoless double-decays ($\beta\beta_{0\nu}$) in nuclear transitions. If $\beta\beta_{0\nu}$ decays are caused by the interaction of light Majorana neutrinos, the amplitude is proportional to the "*effective Majorana mass*" $m_{\ell\ell} = \sum_i U^2_{\ell\nu_i} m_{\nu_i}$, where $U_{\ell\nu_i}$ are the elements of the neutrino-mixing matrix and the sum runs over all neutrino mass eigenstates m_{ν_i}. Consequently, the non-observation of $\beta\beta_{0\nu}$ in nuclear decays sets limits on the effective Majorana mass and restricts new physics scenarios.

In this thesis, we are interested in the complementary study of $\beta\beta_{0\nu}$ decays of hyperons. The motivation for the study of these transitions relies on the cleaner way to compute them, theoretically speaking, than nuclear transitions. Nuclei are rather complicated many body systems and the large number of degrees of freedom leave us with strong model-dependence in the evaluation of the nuclear matrix elements. On the other hand, there are good agreement between calculations of the form factors [8, 9] that describe $\beta\beta_{0\nu}$ hyperon processes letting us have more precision on upper limits of parameters like the effective Majorana masses. Furthermore, the Beijing Electron Spectrometer III (BESIII) has accumulated a large dataset of hyperons which are pair-produced in J/Ψ and $\psi(2S)$ decays on the way to improve previous measurements or search for rare radiative, semileptonic, and rare/forbidden hyperon decay channels [10] where they reported its first results on searches of a few LNV hyperon decay channels which includes the upper limit on $\mathrm{BR}(\Xi^- \to p\mu^-\mu^-) \leq 4\times10^{-8}$. Very recently, BESIII, with the data sample of 1.3×10^9 J/Ψ events, set an upper bounds on LNV hyperon decay $\mathrm{BR}(\Sigma^- \to pe^-e^-) \leq 6.7 \times 10^{-5}$ [11].

The first prediction of $\beta\beta_{0\nu}$ decays of hyperons was reported in [12]. This computation was done considering an effective loop model mechanism involving baryons and a Majorana neutrino as intermediate states, and neglecting the effects of the strong interaction. Actually, they considered the vector and axial hadronic transition form factors as constant parameters; however, under such approximation the amplitude has an UV divergent behavior which was manipulated using a simple cut-off procedure.

Few years later another prediction by the same authors based on the so-

called Massachusetts Institute of Technology (MIT) bag model was presented in [13]. This approach avoids the loop computation over the momenta of the intermediate states, which in principle requires the knowledge of the hadronic form factors at very high energy scales. The results of these two previous computations are rather different. For example, according to the numbers reported in such references, the branching fraction of the $\Sigma \to p e^- e^-$ decay in the MIT bag model (10^{-23}) is around ten orders of magnitude greater than their prediction in the loop model (10^{-33}).

Our main goal is to provide a reliable estimation for the $\beta\beta_{0\nu}$ decays of hyperons in the one-loop model mechanism by including the q^2-dependence of the hadronic transition form factors in the loop integral curing the UV divergent behavior present in [13]. Owing to we are not considering any approximation on the neutrino mass for the loop integrals, we extend the phenomenological analysis including the effects of heavy Majorana masses in the so-called low-scale seesaw models. Additionally, we include all the possible channels involving muons and electrons as final states for the first time.

The structure of the rest of this manuscript is as follows. Chapter I and Chapter II are devoted to present an introduction to the physics and concepts of massive neutrinos and double beta decay, respectively. The relevant computation and numerical analysis of $\beta\beta_{0\nu}$ hyperon decays is presented in Chapter III. Finally, Conclusions and perspectives are presented in Chapter IV. Finally, the Feynman rules for Majorana particles, definitions of the loop integral, and useful formulas relevant in our analysis are reported for completeness in the appendices.

Chapter 1

Massive Neutrinos

This chapter aims to present an overview of massive neutrinos. We are not intended to give an exhaustive review of the theoretical and phenomenological aspects of the neutrino physics, for that goal we refer the reader to excellent reviews given in references [14–16]. Let us start by reviewing the general concepts for Weyl, Dirac and Majorana spinors. After that we will discuss the neutrino oscillation phenomenon and the mixing parameters associated. Finally, we present the different types of realizations of the so-called seesaw mechanism.

1.1 Weyl, Dirac, and Majorana spinors

In 1928, Paul Dirac formulated a relativistic wave function for a free electron (spin 1/2) considering the Schrödinger equation

$$i\frac{\partial\psi}{\partial t} = H\psi, \tag{1.1}$$

and assuming a Hamiltonian of the form

$$H\psi = \left(\vec{\alpha}\cdot\vec{p} + \beta m\right), \tag{1.2}$$

where m is the mass of the electron and $\vec{p}$ its momentum, whereas α and β are hermitian coefficients. Because ψ should also satisfy the relativistic energy-momentum relation

$$H^2\psi = (\mathbf{p}^2 + m^2)\psi, \tag{1.3}$$

the α and β coefficients must fulfill the relations

$$\begin{gathered}\beta^2 = 1, \quad \alpha_1^2 = \alpha_2^2 = \alpha_3^2 = 1, \\ \alpha_i\alpha_j + \alpha_j\alpha_i = 0, \text{for}\, i \neq j, \quad \text{and} \quad \alpha_i\beta + \beta\alpha_i = 0, \text{ for}\, i = 1,2,3.\end{gathered} \tag{1.4}$$

Thus α and β should be associated to 4×4 matrices and ψ is a four component column function.

The Dirac equation can be conveniently written in a symmetric form as follows ($\gamma_0 = \beta$, $\gamma^i = \beta\alpha_i$ for $i = 1, 2, 3$):

$$(i\gamma^\mu\partial_\mu - m)\,\psi = 0, \tag{1.5}$$

which will be regarded as a field equation derived from the action principle of the Lagrangian

$$\mathcal{L} = \bar{\psi}\,(i\gamma^\mu\partial_\mu - m)\,\psi, \tag{1.6}$$

where $\bar{\psi} \equiv \psi^\dagger\gamma_0$, and γ_μ denoting the set of Dirac matrices satisfying the algebra

$$\{\gamma_\mu, \gamma_\nu\} = 2g_{\mu\nu}, \quad \text{and} \quad \gamma_0\gamma_\mu\gamma_0 = \gamma_\mu^\dagger, \tag{1.7}$$

with $\{\gamma_\mu, \gamma_\nu\} \equiv \gamma_\mu\gamma_\nu + \gamma_\nu\gamma_\mu$ stands for the anticommutator. So, any solution of equations (1.2) or (1.5) is called a fermion field, whereas a spinor will denote any column-like function of momentum and energy which when is multiplied by a factor $\exp^{ip.x}$ or $\exp^{-ip.x}$ turns out into a solution of Dirac equation.

1.1.1 Weyl spinors: massless fermions

Note that for massless fermions equations (1.2) and (1.3) are simplified in such a way that the conditions in (1.4) can be identified with the 2×2 Pauli matrices $\vec{\sigma} = (\sigma_1, \sigma_2, \sigma_3)$. Thus the assignation $\vec{\alpha} = \pm\vec{\sigma}$ are two possible solutions of a massless fermion and the Dirac equation can be divided in two independent differential equations

$$\begin{aligned} E\chi &= -\vec{\sigma}\cdot\vec{p}\chi, \\ E\phi &= +\vec{\sigma}\cdot\vec{p}\,\phi, \end{aligned} \tag{1.8}$$

where E is the energy of the particle. The above expressions are known as the Weyl equations and its solutions χ and ϕ are called Weyl spinors. Notice that defining the helicity operator as $\frac{1}{2}\vec{\sigma}\cdot\hat{p}$, for a positive energy the χ (ϕ) spinor has negative (positive) helicity,

1.1.2 Dirac vs Majorana: massive fermions

For a massive fermion, eq. (1.5) is described in terms of the set of the 4×4 Dirac matrices[1], and, in general, if any other restriction is considered,

[1]Notice that the election of the γ_μ matrices is not unique and different bases can be useful to illustrate different aspects of the theory.

the ψ field has in general four independent solutions. In this case, the 4-component column field ψ is called a Dirac spinor. The general rules for the transformation of a Dirac spinor and its adjoint conjugate field under Lorentz transformations are in general independent of the base election for the γ_μ matrices, a detailed explanation of this topic can be found in [17]. Here we concentrate, by the moment, on the description of the antiparticle. From the Klein-Gordon equation we know that there have to be two separate solutions: one for particle ψ and one for antiparticle ψ^c. The ψ^c field is constructed by the transformation

$$\psi \to \psi^c = C\bar{\psi}^T, \tag{1.9}$$

where C is the charge conjugation matrix obeying the relations

$$C^{-1}\gamma_\mu C = -\gamma_\mu^T, \quad C^\dagger = C^T = C^{-1} = -C, \tag{1.10}$$

and we will see that the charge conjugation flips the chirality of the field. From now on, a Majorana fermion can be defined as a solution of the Dirac equation that obeys the condition

$$\psi = \eta\psi^c, \tag{1.11}$$

where η satisfies that $|\eta|^2 = 1$ and is associated to a phase factor proportional to the CP-parity, $\eta = -i\eta_{CP}$. This means that up to this phase η, a Majorana particle is equal to its antiparticle and turns out clear that they cannot have neither electric charge, nor any other numbers associated with a $U(1)$ symmetry.

Now, it turns out convenient to rewrite a fermion field in terms of its left and right components as follows

$$\psi = \psi_L + \psi_R, \quad \text{with} \quad \psi_{\{L,R\}} = P_{\{L,R\}}\psi, \tag{1.12}$$

where $P_{\{L,R\}} \equiv \frac{1}{2}(1 \mp \gamma_5)$ are the left and right-hand projection operator. In this way, it turns out clear to realize that the four independent components of a Dirac field are associated to two left and right chirality states for particle and for the antiparticle

$$\psi_L = P_L\psi, \quad \psi_R = P_R\psi, \quad \psi_L^c \equiv (\psi_L)^c = P_R\psi^c, \quad \psi^c \equiv (\psi_R)^c = P_L\psi^c. \tag{1.13}$$

Whereas, due to the condition $\psi^c = \eta\psi$, a Majorana fermion only has two independent components

$$\psi_L = \eta^*\psi_R^c, \quad \psi_R = \eta\psi_L^c. \tag{1.14}$$

Furthermore, from equations (1.5), (1.13), and (1.14) we can see that a mass term for a fermion field can be written in terms of all the different possible scalar bilinear combinations as follows:

$$\bar{\psi}_L\psi_R = \bar{\psi}^c_R\psi^c_L, \quad \bar{\psi}_R\psi_L = \bar{\psi}^c_L\psi^c_R \quad (\Delta L = 0) \tag{1.15}$$

$$\left.\begin{array}{ll} \bar{\psi}_L\psi^c_L, & \bar{\psi}^c_L\psi_L \\ \bar{\psi}_R\psi^c_R, & \bar{\psi}^c_R\psi_R \end{array}\right\} \quad (\Delta L = 2). \tag{1.16}$$

Note that a Dirac mass term connects L and R components of the same field

$$-\mathcal{L}_D = m_D\bar{\psi}_R\psi_L + \text{h.c.}, \tag{1.17}$$

whereas a Majorana mass term connects L and R components of the conjugate fields

$$-\mathcal{L}_M = \frac{1}{2}m_L\bar{\psi}^c_L\psi_L + \frac{1}{2}m_R\bar{\psi}^c_R\psi_R + \text{h.c.} \tag{1.18}$$

At this point, it is important to mention that in the SM the left-handed components of fermions are accommodated in SU(2)-doublets, whereas the right-handed fields, transform as singlets under the same group of symmetry, except for neutrinos which are not incorporated and as a consequence they are massless particles. For the rest of the fermions, note that the Dirac masses described by the eq. (1.17) are not a gauge-invariant in a direct way, they will be generated by the Higgs mechanism via Yukawa couplings after the Spontaneous Symmetry Breaking (SSB). If right-hand fields for neutrinos are incorporated besides the Dirac mass terms generated after the SSB they will be the unique particles that allow Majorana mass terms.

1.2 Neutrinos flavor mixing

Analogous to the quark sector, if neutrinos are in fact massive particles, there is a mixing between flavor and mass eigenstates, that is, the physical neutrino states can be expressed as a linear combination of flavor eigenstates and vice versa. For the case of only three 3 light Majorana neutrinos ν_i $(i = 1, 2, 3)$, this relation is described by a 3×3 unitary matrix:

$$|\nu_\alpha\rangle = \sum_i \mathbf{U}_{\alpha i}\,|\nu_i\rangle \quad \text{with} \quad \alpha = e, \mu, \tau, \tag{1.19}$$

where α and i stand for the flavor and mass eigenstates, respectively, whereas $\mathbf{U}$ is called the Pontecorvo-Maki-Nakagawa-Sakata matrix (PMNS) [18]. The

PMNS matrix can be parameterized as follows [2]:

$$\mathbf{U}_{\alpha i} = \begin{pmatrix} \mathbf{U}_{e1} & \mathbf{U}_{e2} & \mathbf{U}_{e3} \\ \mathbf{U}_{\mu 1} & \mathbf{U}_{\mu 2} & \mathbf{U}_{\mu 3} \\ \mathbf{U}_{\tau 1} & \mathbf{U}_{\tau 2} & \mathbf{U}_{\tau 3} \end{pmatrix} = \mathbf{O} \begin{pmatrix} e^{\alpha_1} & 0 & 0 \\ 0 & e^{\alpha_2} & 0 \\ 0 & 0 & 1 \end{pmatrix}, \tag{1.20}$$

with

$$\begin{aligned} \mathbf{O} &= \begin{pmatrix} 1 & 0 & 0 \\ 0 & c_{23} & s_{23} \\ 0 & -s_{23} & c_{23} \end{pmatrix} \begin{pmatrix} c_{13} & 0 & e^{-i\delta_{13}} s_{13} \\ 0 & 1 & 0 \\ -e^{i\delta_{13}} s_{13} & 0 & c_{13} \end{pmatrix} \begin{pmatrix} c_{12} & s_{12} & 0 \\ -s_{12} & c_{12} & 0 \\ 0 & 0 & 1 \end{pmatrix} \\ &= \begin{pmatrix} c_{12}c_{13} & s_{12}c_{13} & s_{12}e^{-i\delta_{13}} \\ -s_{12}c_{23} - c_{12}s_{23}s_{13}e^{i\delta_{13}} & c_{12}c_{23} - s_{12}s_{23}s_{13}e^{i\delta_{13}} & s_{23}c_{13} \\ s_{12}s23 - c_{12}c_{23}s_{13}e^{i\delta_{13}} & -c_{12}s_{23} - s_{12}c_{23}s_{13}e^{i\delta_{13}} & c_{23}c_{13} \end{pmatrix}, \end{aligned} \tag{1.21}$$

and the notation $c_{ij} \equiv \cos\theta_{ij}$ and $s_{ij} \equiv \sin\theta_{ij}$ has been introduced. Note that the second diagonal matrix in eq. (1.20) is associated to the Majorana phases which cannot be avoided using a redefinition of the fields. The values for all the parameters appearing in (1.21) are determined experimentally, and can be found in [19], except for the Majornana phases. These phases are not experimentally sensitive, at least through the neutrino oscillations phenomenon. Therefore, in order to distinguishes the Majorana nature of neutrino there would be necessary the observation of a lepton number violating process.

1.3 Neutrinos vacuum oscillation

Neutrino oscillation is a quantum phenomenon confirmed by several experiments where a neutrino of flavor ν_α ($\alpha = e, \mu, \tau$) that has been created in a charged weak current interaction can be detected with a different flavor after its distance propagation. The first studies on this phenomenon were presented in ref. [20]. From quantum mechanics we know that the temporal evolution of a "*flavor*" state $|\nu_\alpha(t)\rangle$ is described by

$$|\nu_\alpha(t)\rangle = \Theta(t - t_0)\,|\nu_\alpha(t_0)\rangle = \sum_i \mathbf{U}_{\alpha i} e^{i\mathcal{H}t}\,|\nu_i(0)\rangle\,, \tag{1.22}$$

where $|\nu_i\rangle$ represents the physical states (states with a well defined energy $\mathcal{H}\,|\nu_i\rangle = E_i\,|\nu_i\rangle$), and $\mathbf{U}_{\alpha_i}$ are the mixing matrix elements reviewed on pre-

[2] Note that in the case of Dirac fields the second diagonal matrix in (1.20) is actually the unit matrix.

vious section. Thus, we can rewrite the above equation as follows:

$$|\nu_\alpha(t)\rangle = \sum_i \mathbf{U}_{\alpha i} e^{-iE_i t} |\nu_i(0)\rangle . \tag{1.23}$$

Thus the probability that after a time t the $|\nu_\alpha\rangle$ state oscillates to $|\nu_\beta\rangle$ is given by

$$\begin{aligned} |\langle\nu_\beta|\nu_\alpha\rangle|^2 &= \left| \sum_{ji} \langle\nu_j| \mathbf{U}^*_{\beta j}\mathbf{U}_{\alpha i} e^{-iE_i t} |\nu_i\rangle \right|^2 \\ &= \left| \sum_i \mathbf{U}^*_{\beta i}\mathbf{U}_{\alpha i} e^{-iE_i t} \right|^2 \\ &= \left| \sum_i \mathbf{U}^*_{\beta i}\mathbf{U}_{\alpha i} e^{-i\frac{m_i^2 L}{2p}} \right|^2 \\ &= \sum_i \mathbf{U}^*_{\beta i}\mathbf{U}_{\alpha i} e^{-i\frac{m_i^2 L}{2p}} \sum_j \mathbf{U}_{\beta j}\mathbf{U}^*_{\alpha j} e^{i\frac{m_i^2 L}{2p}} \\ &= \sum_{ij} \mathbf{U}^*_{\beta i}\mathbf{U}_{\alpha i}\mathbf{U}_{\beta j}\mathbf{U}^*_{\alpha j} e^{-i\frac{(m_i^2 - m_j^2)L}{2p}}, \end{aligned} \tag{1.24}$$

where we have used the approximation $t \approx L$ owing to neutrinos are relativistic particles, and L represents the distance traveled for a time t; then, expanding E for $m \ll p$ as follows

$$E = \sqrt{p^2 + m^2} \approx p + \frac{m^2}{2p}. \tag{1.25}$$

Splitting the sum $\sum_i = \sum_{i=j} + \sum_{i<j} + \sum_{i>j}$ in eq. (1.24) and after some algebra, we can write the transition probability:

$$\begin{aligned} |\langle\nu_\beta|\nu_\alpha\rangle|^2 =& \delta_{\alpha\beta} - 4\sum_{i>j} Re\left(\mathbf{U}^*_{\beta i}\mathbf{U}_{\alpha i}\mathbf{U}_{\beta j}\mathbf{U}^*_{\alpha j}\right) \sin^2\left(\frac{\Delta m_{ij} L}{4E}\right) \\ &+ 2\sum_{i>j} Im\left(\mathbf{U}^*_{\beta i}\mathbf{U}_{\alpha i}\mathbf{U}_{\beta j}\mathbf{U}^*_{\alpha j}\right) \sin\left(\frac{\Delta m_{ij} L}{2E}\right), \end{aligned} \tag{1.26}$$

where the approximation $p \approx E$ was considered and we have defined $\Delta m^2_{ji} \equiv m_i^2 - m_j^2$.

For illustrative purposes we consider only two physical states and two flavors. In this situation the mixing $\mathbf{U}$ is well defined as a 2×2 matrix:

$$\mathbf{U} = \begin{pmatrix} \cos\theta & \sin\theta \\ -\sin\theta & \cos\theta \end{pmatrix}. \tag{1.27}$$

Then, from eq. (1.26)

$$\mathcal{P}^{\beta\neq\alpha}_{\alpha\to\beta} = \sin^2(2\theta)\sin^2\left(\frac{\Delta m^2 L}{2E}\right). \tag{1.28}$$

This last expression is often used to describe the transition $\nu_\mu \to \nu_\tau$ in atmospheric mixing, because the electron neutrino does not play any role in this case. Nevertheless, until now we only have considered the propagation as free particles. Oscillations of neutrinos traveling in a medium, can be treated in perturbation theory using interaction potentials to describe the medium [21].

The important point to remark from eq. (1.26) is that oscillation between defined flavor states just happens if $\Delta m \neq 0$, in other words, neutrinos are in fact massive particles. In the framework of three-neutrino flavors, the transition probabilities depend on six independent parameters: θ_{12}, θ_{13}, θ_{23}, δ_{13}, Δm^2_{23} and Δm^2_{12} (see table 1.1), and there are two different scenarios for the mass ordering:

- Normal Hierarchy (NH)

In this case we have $m_1 \ll m_2 \ll m_3$. It let us write $m_{1,2}$ in terms of squared-mass differences as follow:

$$\begin{aligned}\sqrt{\Delta m^2_{12}} &= \sqrt{m_2^2 - m_1^2} \approx m_2,\\ \sqrt{\Delta m^2_{23}} &= \sqrt{m_3^2 - m_2^2} \approx m_3.\end{aligned} \tag{1.29}$$

- Inverted Hierarchy (IH)

The hierarchy in this case is given by $m_3 \ll m_1 \lesssim m_2$, hence:

$$\sqrt{|\Delta m^2_{13}|} = \sqrt{m_1^2 - m_3^2} \approx m_1, \tag{1.30}$$

and

$$\begin{aligned} m_2 \approx \sqrt{\Delta m^2_{23}} &= \sqrt{\Delta m^2_{12} + |\Delta m^2_{13}|},\\ &= \sqrt{|\Delta m^2_{13}|}\left(1 + \frac{\Delta m^2_{12}}{|\Delta^2_{13}|}\right)^{1/2},\\ &\approx \sqrt{|\Delta m^2_{13}|}\left(1 + \frac{\Delta m^2_{12}}{2|\Delta m^2_{13}|}\right). \end{aligned} \tag{1.31}$$

Parameters	Normal Hierarchy (NH)	Inverted Hierarchy (IH)
$\sin^2\theta_{12}$	$0.304^{+0.013}_{-0.012}$	$0.304^{+0.013}_{-0.012}$
$\theta_{12}/^\circ$	$33.44^{+0.78}_{-0.75}$	$33.44^{+0.78}_{-0.75}$
$\sin^2\theta_{23}$	$0.57^{+0.018}_{-0.024}$	$0.575^{+0.017}_{-0.75}$
$\theta_{23}/^\circ$	$49.0^{+1.1}_{-1.4}$	$49.3^{+1.0}_{-1.2}$
$\sin^2\theta_{13}$	$0.02221^{+0.00068}_{-0.00062}$	$0.02240^{0.00062}_{0.00062}$
$\theta_{13}/^\circ$	$8.57^{+0.13}_{-0.12}$	$8.61^{+0.12}_{-0.12}$
$\delta_{12}/^\circ$	195^{+51}_{-12}	286^{+27}_{-32}
$\Delta m^2_{12}/10^{-5}\text{eV}^2$	$7.42^{+0.21}_{-0.20}$	$7.42^{+0.21}_{-0.20}$
$\Delta m^2_{31}/10^{-3}\text{eV}^2$	$+2.514^{+0.028}_{-0.027}$	$-2.497^{+0.028}_{-0.028}$

Table 1.1: Three-flavor neutrino oscillation parameters taken from ref. [19].

1.4 Seesaw mechanism

We have seen that the experimental evidence of neutrino oscillation implies that neutrinos are indeed massive particles and requires to modify the original formulation of the SM. The simplest way to solve this problem is just adding right-handed field (ν_R) to the theory in order to generate Dirac masses via Yukawa couplings with the Higgs doublet, just like for all the other fermions. Nevertheless, once we introduce right-handed neutrinos there are no impediments that prohibit the inclusion of a Majorana mass term ($\frac{1}{2}m_R\bar{\nu^c_R}\nu_R$) as well. Moreover, as we will discuss later, under extra considerations some models may admit left-handed Majorana masses too. Then let us consider the case of only one neutrino family with the most general mass term given by

$$\begin{aligned}
-\mathcal{L}_m =& \frac{1}{2}\left(2m_D\bar{\nu}_L\nu_R + m_L\bar{\nu^c_L}\nu_L + m_R\bar{\nu^c_R}\nu_R + h.c\right) \\
=& \frac{1}{2}\left(\bar{\nu^c_L}, \bar{\nu_R}\right)\begin{pmatrix} m_L & m_D \\ m_D & m_R \end{pmatrix}\begin{pmatrix} \nu_L \\ \nu^c_R \end{pmatrix} + h.c \\
=& \frac{1}{2}\left(\bar{\nu^c_L}, \bar{\nu_R}\right) M \begin{pmatrix} \nu_L \\ \nu^c_R \end{pmatrix} + h.c.,
\end{aligned} \tag{1.32}$$

the neutrino mass M can be diagonalized by a unitary transformation [3], such that

$$M' = U^T M U = \begin{pmatrix} m'_1 & 0 \\ 0 & m'_2 \end{pmatrix}, \tag{1.33}$$

[3]Further details can be found in ref. [22].

where U can be defined as:

$$U = O\rho \quad \text{with} \quad O = \begin{pmatrix} \cos\theta & \sin\theta \\ -\sin\theta & \cos\theta \end{pmatrix}; \quad \rho = \begin{pmatrix} \rho_1 & 0 \\ 0 & \rho_2 \end{pmatrix}, \tag{1.34}$$

with $\rho_{1,2}^2 = \mp 1$ and $\tan\theta = 2m_D/(m_R - m_L)$. The eigenvalues for M are

$$m_{1,2} = \frac{(m_L + m_R) \mp \sqrt{(m_L - m_R)^2 + 4m_D^2}}{2}, \tag{1.35}$$

in such that the physical masses in eq. (1.33) can be written as $m'_{1,2} = \rho_{1,2}^2 m_{1,2}$. Now, the generalization of this problem to a scenario with n left-handed and k right-handed neutrinos leads us to diagonalize a block matrix $(n+k) \times (n+k)$ given by

$$\tilde{M} = \begin{pmatrix} m_{L_{n\times n}} & m^T_{D_{n\times k}} \\ m_{D_{k\times n}} & m_{R_{k\times k}} \end{pmatrix}. \tag{1.36}$$

However, since $\tilde{M}$ is still a complex symmetric matrix, the diagonalization is again obtained through a unitary transformation ($\mathbf{U}$). In general $\mathbf{U}$ is the so-called mixing matrix, because it lets us write the chiral fields as a linear combination of the mass eigenstates (ν_i) such that

$$\nu_{iL} = \sum_j^{n+k} \mathbf{U}_{ij}\nu_j, \quad \nu^c_{iR} = \sum_j^{n+k} \mathbf{U}_{ij}\nu_j. \tag{1.37}$$

1.4.1 Type I

The type-I seesaw mechanism is based on three main assumptions. First, $m_L = 0$ in eq. (1.32). Second, the Dirac masses are generated by the Higgs mechanism, then m_D should be of the order of the electroweak scale. Third, m_R must be much larger than m_D ($m_D \ll m_R$). Thus, with all this we can rewrite eq. (1.35) as follows

$$m_{1,2} = \frac{m_R}{2}\left(1 \mp \sqrt{1 + \left(\frac{2m_D}{m_R}\right)^2}\right). \tag{1.38}$$

Now, using series expansion for the limit $m_D \ll m_R$

$$\begin{aligned} m'_1 =& -\frac{m_R}{2}\left(1 - \left[1 + \frac{1}{2}\left(\frac{2m_D}{m_R}\right)^2 + \mathcal{O}\left(\frac{2m_D}{m_R}\right)\right]\right) \\ \approx& \frac{m_D^2}{m_R}. \end{aligned} \tag{1.39}$$

$$\begin{aligned} m_2' =& \frac{m_R}{2}\left(1+\left[1+\frac{1}{2}\left(\frac{2m_D}{m_R}\right)^2+\mathcal{O}\left(\frac{2m_D}{m_R}\right)\right]\right) \\ \approx& m_R\left(1-\frac{m_D^2}{m_R^2}\right)\approx m_R. \end{aligned} \tag{1.40}$$

Setting $m_D \sim 200$ GeV and $m_R \sim 10^{15}$ GeV around the grand unification scale, in eqs. (1.39) and (1.40) we can conclude that physical mass m_1 is very suppressed $(10^{-2}-10^{-1})$eV as it happens for the active neutrinos masses in oscillation experiments. On the contrary, the second massive particle, the so-called sterile neutrino has a mass $\sim 10^{15}$ GeV. The eigenvectors are:

$$\begin{aligned} \nu_1 =& (\nu_L+\nu_L^c)-\frac{m_D}{m_R^2}(\nu_R+\nu_R^c), \\ \nu_2 =& \frac{m_D}{m_R^2}(\nu_L+\nu_L^c)+(\nu_R+\nu_R^c). \end{aligned} \tag{1.41}$$

From eq. (1.41) we can see that the light neutrino m_1 is mostly composed of $\nu_L+\nu_L^c$ because the $\nu_R+\nu_R^c$ component is suppressed by a factor m_D/m_R^2. In contrast, the state m_2 is suppressed on the component $\nu_L+\nu_L^c$ by the same factor.

1.4.2 Type II

Now we may wonder what happens if we take eq. (1.35) with $m_L \neq 0$. To do this we need to add to the SM a $SU(2)_L$ triplet scalar field h in addition to the doublet Higgs field ϕ, in order to admit left-handed Majorana mass terms, as is shown on [24].

$$h=\begin{pmatrix} H^0 & H^-/\sqrt{2} \\ H^-/\sqrt{2} & H^{--} \end{pmatrix}; \quad \phi=\begin{pmatrix} \phi^+ \\ \phi^0 \end{pmatrix}, \tag{1.42}$$

and the corresponding Yukawa coupling term add to the Lagrangian

$$\mathcal{L}=\sum_{a,b} g_{a,b}\Psi_a^T \mathbf{C}^{-1}\tau_2 h \Psi_b + h.c., \tag{1.43}$$

in order to get a left-handed Majorana mass term after spontaneous symmetry breaking. This is the so-called seesaw type II seesaw mechanism, where physical state masses are described by using the approximation $m_L, m_D \ll m_R$ on eq. (1.35) such that:

$$\begin{aligned} m_1 \approx& m_L - m_D^T m_R^{-1} m_D \\ m_2 \approx& m_R. \end{aligned} \tag{1.44}$$

1.4.3 Type III

Finally, the seesaw type III involves the addition of a new $SU(2)_L$ fermion triplet [25]

$$\Sigma_R = \begin{pmatrix} \Sigma_R^0/\sqrt{2} & \Sigma_R^+ \\ \Sigma_R^- & -\Sigma_R^0/\sqrt{2} \end{pmatrix}. \tag{1.45}$$

Their interactions are described by the following terms in the Lagrangian

$$-\mathcal{L}_\Sigma = \Phi^\dagger \bar{\Sigma}_R \sqrt{2} Y_\Sigma L + \frac{1}{2} Tr[\bar{\Sigma}_R M \Sigma_R^c] + h.c, \tag{1.46}$$

where for simplicity we have omitted generational indices, Y_Σ is a Yukawa coupling, and L is the usual $SU(3)_L$ doublet (l^-, ν). After the spontaneous symmetry breaking, and analogous to the type-I scenario the light neutrino mass is given by $m_\nu \sim \frac{Y_\Sigma Y_\Sigma^T}{m_\Sigma}$.

Chapter 2

Double beta decay

It is well known that neutrino oscillation phenomena are not sensitive to Majorana neutrinos. The Majorana nature of neutrinos can be established only via searches of processes which break lepton number. This chapter is devoted to discuss the most important aspects of double beta decays in nuclei, which are the most sensitive laboratory in the search of lepton number violating effects. We present the differences between neutrinoless ($\beta\beta_{0\nu}$) and two neutrino double beta decays ($\beta\beta_{2\nu}$), where the latter can be triggered independently of the non-zero masses and nature of neutrinos. Later we discuss the conditions required for the existence of $\beta\beta_{0\nu}$ decays and some of their possible mechanisms. Finally, we review briefly the current limits on the effective Majorana mass - a relevant parameter in the study of $\beta\beta_{0\nu}$ transitions.

2.1 Two neutrino double beta decay $\beta\beta_{2\nu}$

The existence of $\beta\beta_{2\nu}$ was proposed for the first time in the decade of the 1930's. This process takes place when a nucleus with a number A of nucleons (from which Z are protons) transmutes into another nucleus with Z+2 protons emitting two electrons and two anti-neutrinos, that is:

$$(Z, A) \rightarrow (Z + 2, A) + e^- e^- + \bar{\nu}_e \bar{\nu}_e. \tag{2.1}$$

The amplitude of these processes is proportional to G_F^2 so they are naturally suppressed but allowed in the SM. They have been observed in fourteen isotopes in direct "counting" experiments [19, 26]. There are two possible mechanisms reported in the literature (see Fig. 2.1): the two nucleus mechanism (2n-) and the so-called N^* mechanism (a detailed explanation of this topic can be found in ref. [27]). The 2n-mechanism is carried out in two different hadronic lines, where in each one, a neutron (n_i) decays into a proton

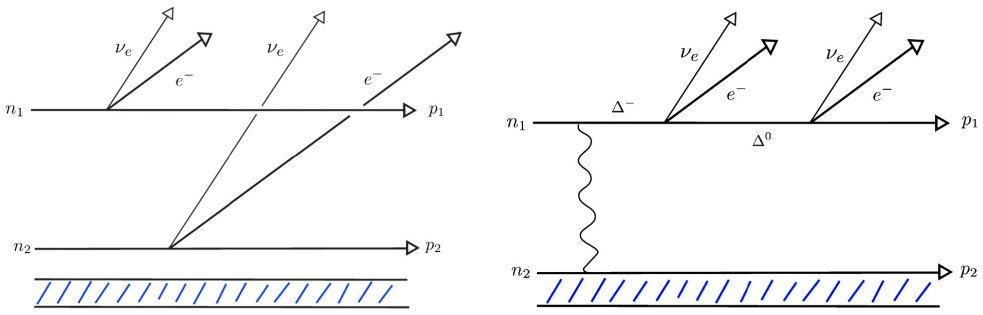

Figure 2.1: Left: $\beta\beta_{(2\nu)}$ in the 2nd-mechanism. Right: $\beta\beta_{(2\nu)}$ in the N^* mechanism. The dashed lines on blue represent the rest of nucleons that do not interact on the process and the wavy line represent a strong interaction.

(p_i) by a simple β decay. On the other hand, the N^* mechanism is produced only in one hadronic line in which the bounded neutron undergoes a double beta decay transition via the decay chain involving $\Delta^{-,0}$ resonances, via the process $\Delta^- \to p + 2e^- + 2\nu_e$, see fig. 2.1.

2.2 $\beta\beta_{0\nu}$ neutrinoless decay ($\Delta L = 2$)

Furry [28] studied for the first time the double beta decay in nuclei without the emission of neutrinos:

$$(Z, A) \to (Z + 2, A) + e^- e^-. \tag{2.2}$$

Of course the above process violates lepton number in two units and is absent to any order in the SM. For this reason, its discovery would be a smoking gun of new physics. The mechanism triggering this transition requires to introduce a Majorana neutrino that is exchanged between two nucleon lines to produce two electrons as shown in fig. 2.3. Now, in order to be allowed are needed two conditions within the SM.

- The electron neutrino must be its own antiparticle ($\nu_e = \nu_e^c$).
- The helicity of the neutrino that is emitted on vertex α on Fig. (2.3) and the one which is absorbed on vertex β need to be the same.

The basic process that generates $\beta\beta_{0\nu}$ decays triggered by Majorana neutrinos is shown by fig. 2.2. Different physical processes involves this kernel or its crossed diagram. When incorporating the currents for production or decay

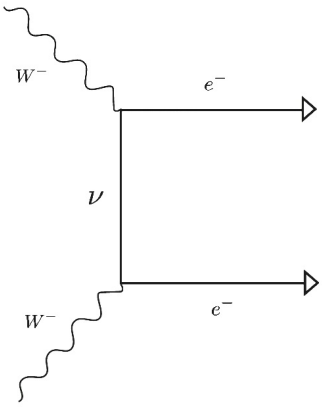

Figure 2.2: $\beta\beta_{0\nu}$ fundamental kernel.

of W gauge bosons, the amplitude becomes of $O(G_F^2)$ yielding a strong suppression factor. It should be mentioned that, similar to $\beta\beta_{2\nu}$ decay, we could have neutrinoless double beta decays via the N^* mechanism, as is shown on Fig. (2.3). Here, the transition happens by the process $\Delta^- \to \Delta^+ e^- e^-$ with the neutrino and the hadronic intermediate state Δ^0 inside the loop. Nevertheless, these scenarios are even more suppressed than 2n-mechanism.

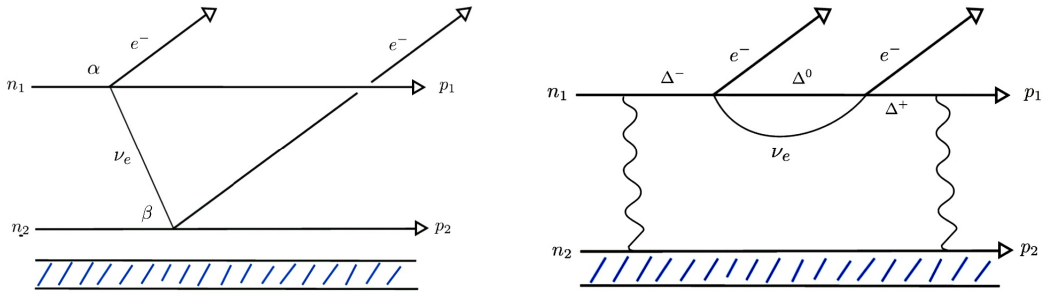

Figure 2.3: Right: $\beta\beta_{(0\nu)}$ decay in the N^* mechanism. The dashed lines on blue represent the rest of nucleons that do not interact on the process and the wavy lines represent a strong interaction. Left: $\beta\beta_{0\nu}$ disintegration in the 2n-mechanism.

2.3 Experimental searches of $\beta\beta$ decays in nuclei

Experiments on double beta decay consists in the observation of the two electrons emitted in nuclear transitions which are forbidden via simple beta decay but allowed via $\beta\beta_{2\nu}$ or $\beta\beta_{0\nu}$ as is illustrated on Fig. (2.4), being the most used isotopes: ${}^{48}_{20}$Ca, ${}^{76}_{32}$Ge, ${}^{82}_{32}$Se, etc. The way to distinguish $\beta\beta_{2\nu}$ from $\beta\beta_{0\nu}$ decays is given by sum of the energies T of the two emitted electrons: while the processes with two neutrinos have a continuous spectrum, neutrinoless decays have a fixed energy T given by the signature $Q = m_i - m_f - 2m_e$ as is shown in the right hand side of Fig. (2.4). Current bounds for the half-life time of different nuclear $\beta\beta_{0\nu}$ disintegrations are reported on Table 2.1. As we can see, this kind of transitions are really suppressed, with lower limits around $\sim 10^{21}$ years.

Isotope	$T^{0\nu}_{1/2}$ $[10^{25} years]$	Experiment
^{48}Ca	$> 5.8 \times 10^{-3}$	ELEGANT-IV
^{76}Ge	> 8.0	GERDA
	> 1.9	MAJORANA DEMONSTRATOR
^{82}Se	$> 3.6 \times 10^{-2}$	NEMO-3
^{92}Zr	$> 9.2 \times 10^{-4}$	NEMO-3
^{100}Mo	$> 1.1 \times 10^{-1}$	NEMO-3
^{116}Cd	$> 2.2 \times 10^{-2}$	Aurora
^{128}Te	$> 1.1 \times 10^{-2}$	C. Arnaboldi et al.
^{130}Te	> 1.5	CUORE
^{136}Xe	> 10.7	KamLAND-Zen
	> 1.8	EXO-200
^{150}Nd	$> 2.0 \times 10^{-3}$	NEMO-3

Table 2.1: Half-life time of nuclear $\beta\beta_{0\nu}$ desintegrations reported on Ref. [29].

2.4 Alternative schemes for $\beta\beta_{0\nu}$

There are other frameworks that discuss the possibility of having $\beta\beta_{0\nu}$ decays, without requiring to introduce massive Majorana neutrinos; some of them are reviewed on ref. [27]. In the following we briefly comment these alternative frameworks. However, we stress that, the work of Schechter and Valle in

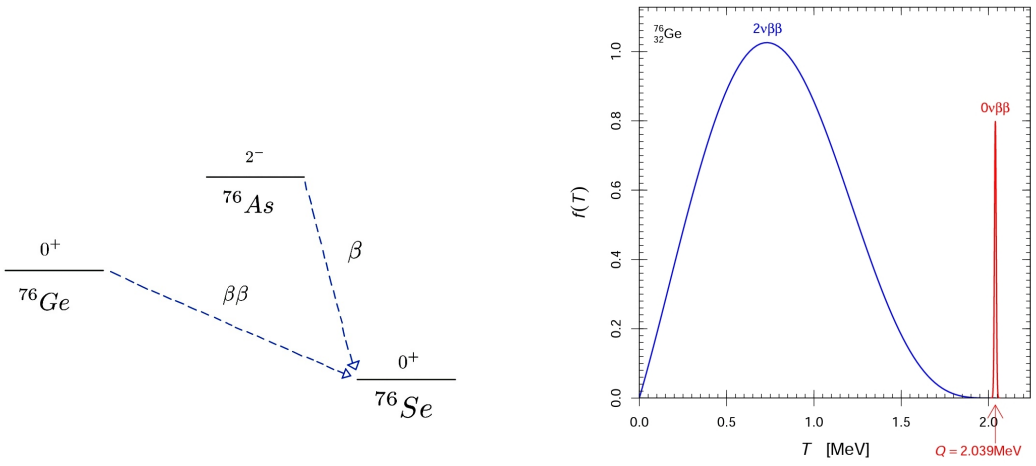

Figure 2.4: Left: $\beta\beta_{(0\nu)}$ transition for ^{76}Ge. Right:Energy spectrum for emitted electrons on $^{76}_{32}$Ge double beta decay taken from ref. [30].

ref. [31], derives a theorem (that bears their names) which states that in a gauge theory the detection of neutrinoless double beta decays implies the Majorana nature of neutrinos.

2.4.1 $\beta\beta$ decay mediated by Higgs bosons

Some models predict the existence of doubly charged Higgs bosons that couple to two electrons, and allowing a $\beta\beta_{0\nu}$ decay as is shown in the upper-left fig.2.5. Summarizing [32], the authors used an extended model where a $SU(2)_L$- triplet Higgs boson (H) is added in order to generate a left-handed Majorana mass term for neutrinos via the Type II seesaw mechanism. Here, the Yukawa compling between leptons and this new triplet is given by

$$-\mathcal{L}_Y = \sum_{ij} h_{l,l'} \bar{\psi}^c_{\ell L} H^\dagger \psi_{\ell L} + h.c., \tag{2.3}$$

taking

$$H = \begin{pmatrix} H^0 & H^-/\sqrt{2} \\ H^-/\sqrt{2} & H^{--} \end{pmatrix}; \quad \psi_{\ell L} = \begin{pmatrix} \ell^-_L \\ \nu_L \end{pmatrix}. \tag{2.4}$$

Along the same line, once this new field is added to the theory, it becomes possible to add a coupling between this triplet H and the well-known Higgs boson doublet ϕ as follows.

$$\mathcal{L}_I = m_H \phi^\dagger H \phi + h.c. \tag{2.5}$$

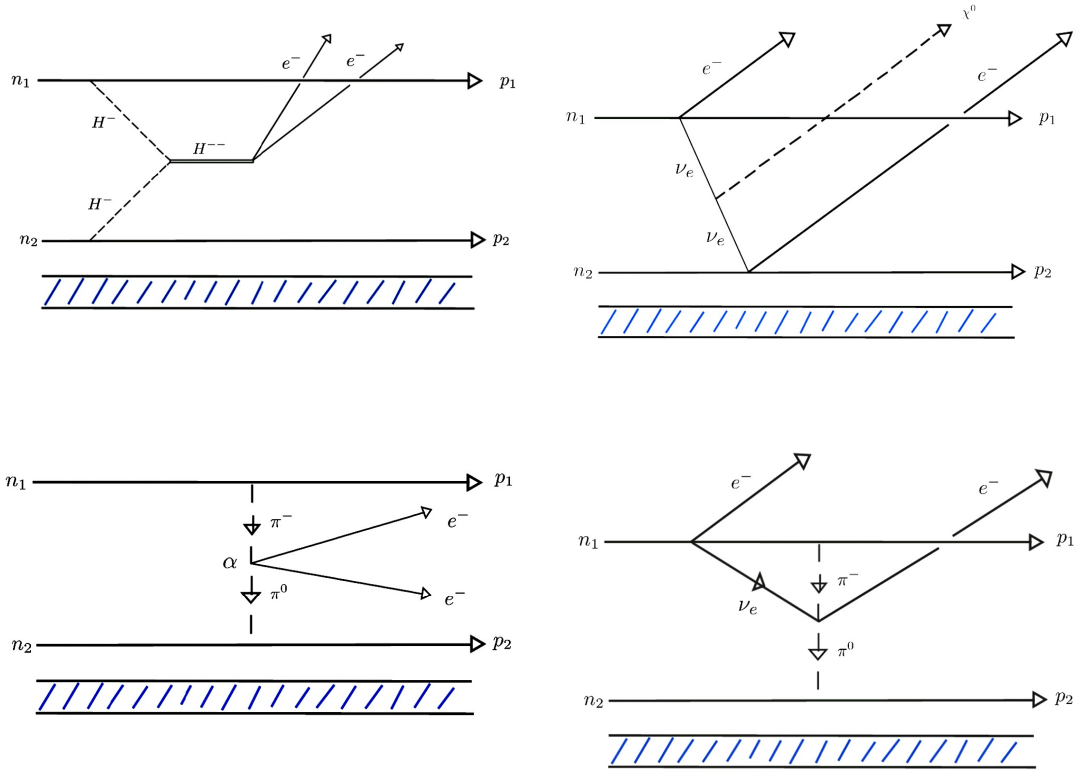

Figure 2.5: Alternative schemes for $\beta\beta_{0\nu}$ nuclei decays. Upper-left: Induced by double charged Higgs boson. Upper-right: Induced by a Majoron. Lower-left: Induced by pions, Lower-right: Induced by pions in the 2n-mechanism.

The above interaction let us write a new contribution to the $\beta\beta_{0\nu}$ decay given by the upper-left process in fig. 2.5. However, the amplitude of this transition is suppressed by a factor $(v_H/v_\phi)^2 \sim 10^{-20}$ where v_H and v_ϕ are the vacuum expectation values of the fields H and ϕ, respectively. Furthermore, the matrix element will get suppressed too, letting us to neglect this contribution.

2.4.2 Majoron emitting process

A different way to produce $\beta\beta_{0\nu}$ is the following:

$$(Z, A) \rightarrow (Z + 2, A) + e^- e^- + \chi^0, \tag{2.6}$$

where χ^0 on the upper-right diagram of fig. 2.5 represents a Majoron particle which is a massless Goldstone boson that appears after the L-B symmetry

breaking. In models as [33], this Majoron particles comes from the coupling of H^0, the neutral component of a triplet Higgs boson, where the effective interaction with neutrinos is given by:

$$\mathcal{L}_{int} = \sum_{ij} g_{ij} \bar{\nu}_j \gamma^5 \nu_j \chi, \tag{2.7}$$

where χ represents the Majoron field. On the other hand, if we suggest that the χ field is given by a $SU(2)_L$-singlet on the way to introduce it without any other interaction beyond the interaction with right-handed neutrinos, then the coupling of this singlet Majoron field to light neutrinos becomes very small due to the smallness of the mixing for right-handed neutrinos.

2.4.3 $\beta\beta_{0\nu}$ mediated by pions

The last contribution to $\beta\beta_{0\nu}$ decays we will comment is related to the exchange of pseudoscalar mesons (π) in the 2n-mechanism to produce neutrinoless double beta decays, as is shown in lower diagrams in fig. 2.5. The first evaluation of the the half-life time for $\beta\beta_{0\nu}$ mediated by pions decays was done in Ref. [34].

2.5 Effective Majorana mass

An important parameter in neutrinoless double beta decays is the so-called *Effective Majorana mass* ($\langle m_{ee} \rangle$) which is defined as:

$$\langle m_{ee} \rangle = \sum_j m_{\nu j} U_{ej}^2, \tag{2.8}$$

(or more generally, $\langle m_{\ell\ell'} \rangle = \sum_j m_{\nu j} U_{\ell j} U_{\ell' j}$ in the case of different lepton flavors ℓ, ℓ' where $U_{\ell j}$ are given by the matrix elements in eq. (1.21). Now, we can use the current experimental values for the parameters shown in Table 1.1 in order to estimate limits on $\langle m_{ee} \rangle$. From eqs. (2.8) and (1.21) we can write the effective Majorana mass as follows

$$\begin{aligned} |\langle m_{ee} \rangle| &= |c_{13}^2 c_{12}^2 e^{2i\alpha_1} m_1 + c_{13}^2 s_{12}^2 e^{2i\alpha_2} m_2 + s_{13}^2 e^{-2i\delta_{12}} m_3| \\ &= |c_{13}^2 c_{12}^2 e^{2i\Delta_1} m_1 + c_{13}^2 s_{12}^2 e^{2i\Delta_2} m_2 + s_{13}^2 m_3|, \end{aligned} \tag{2.9}$$

with $\Delta_i = \alpha_i + \delta_{12}$. Analyzing eq. (2.9) in the two different neutrino masses-ordering schemes reviewed in the previous chapter:

- Normal Hierarchy

Using eq. (1.29) into eq. (2.9) an neglecting the contribution of m_1 we can rearrange $|\langle m_{ee}\rangle|$ as follows:

$$|\langle m_{ee}\rangle| = \left| c_{13}^2 s_{12}^2 e^{2i\Delta_2}\sqrt{\Delta m_{12}^2} + s_{13}^2\sqrt{\Delta m_{23}^2}\right|. \tag{2.10}$$

Now, if we use:

$$\begin{aligned} |ae^{i\delta}+b| &= |a\cos\delta + b + ia\sin\delta| \\ &= \left(a^2+b^2+2ab\cos\delta\right)^{1/2}, \quad \text{with} \quad a,b\in\mathcal{R}\ , \end{aligned} \tag{2.11}$$

then, by identifying $a = c_{13}^2 s_{12}^2\sqrt{\Delta m_{12}^2}$ and $b = s_{13}^2\sqrt{\Delta m_{23}^2}$, we can write eq. (2.10) as follows

$$|\langle m_{ee}\rangle| = \left(c_{13}^4 s_{12}^4\Delta m_{12}^2 + s_{13}^4\Delta m_{23}^2 + 2\cos(2\Delta_2)c_{13}^2 s_{12}^2 s_{13}^2\sqrt{\Delta m_{12}^2\Delta m_{23}^2}\right)^{1/2}. \tag{2.12}$$

Taking the case with $\cos(2\Delta_2)\approx 1$ lets us write an upper bound for $|\langle m_{ee}\rangle|$

$$|\langle m_{ee}\rangle| < c_{13}^2 s_{12}^2\sqrt{\Delta m_{12}^2} + s_{13}^2\sqrt{\Delta m_{23}^2} \approx 4.25\times 10^{-3} eV, \tag{2.13}$$

where we have used the experimental limits for the mixing angles and squared-mass differences within 3σ values from Table 1.1.

- Inverted Hierarchy

In the same way as with the normal hierarchy, taking eqs. (1.30) and (1.31) in eq. (2.9) and neglecting m_3 we can write the effective Majorana mass as:

$$\begin{aligned} |\langle m_{ee}\rangle| &= c_{13}^2\sqrt{\Delta m_{13}^2}|c_{12}^2 e^{2i\Delta_1} + s_{12}^2 e^{2i\Delta_2}| \\ &= c_{13}^2\sqrt{\Delta m_{13}^2}\left|c_{12}^2 e^{2i\Delta} + s_{12}^2\right|, \end{aligned} \tag{2.14}$$

with $\Delta = \Delta_1 - \Delta_2 = \alpha_1 - \alpha_2$. Then, using eq. (2.11) in eq. (2.14) we can write:

$$|\langle m_{ee}\rangle| = c_{13}^2\sqrt{\Delta m_{13}^2}\left(c_{12}^4 + s_{12}^4 + 2\cos(2i\Delta)c_{12}^2 s_{12}^2\right)^{1/2}. \tag{2.15}$$

It is easy to see that the limits on $|\langle m_{ee}\rangle|$ from eq. (2.15) come from the unknown Majorana phase difference Δ. Then in order to set upper and lower bounds we take the values for $\cos(2\Delta) = \pm 1$, what lets us write:

$$c_{13}^2(c_{12}^2 - s_{12}^2)\sqrt{\Delta m_{13}^2} \lesssim |\langle m_{ee}\rangle| \lesssim c_{13}^2\sqrt{\Delta m_{13}^2}. \tag{2.16}$$

Using the values given in Table 1.1 within 3σ, we have

$$1.41 \times 10^{-2} \text{ eV} \lesssim |\langle m_{ee} \rangle| \lesssim 4.51 \times 10^{-2} \text{ eV}. \tag{2.17}$$

The value of $\langle m_{ee} \rangle$ as a function of the lightest neutrino mass (m_{light}) is plotted in Fig.(2.8) for the two different mass-ordering schemes. One of the main conclusions we can draw from this figure is that for the Inverted Hierarchy (IH), $|\langle m_{ee} \rangle|$ can not be zero (region within green lines), independently of the value of Majorana phases α_i. On the other hand, for Normal Hierarchy (NH) the effective Majorana mass can be zero in the interval $m_{light} = (2-7) \times 10^{-3}$ eV, which would lead to vanishing double beta decays. It is important to mention that, even if $\beta\beta_{0\nu}$ are detected, it will not give any information of the hierarchy of neutrino masses.

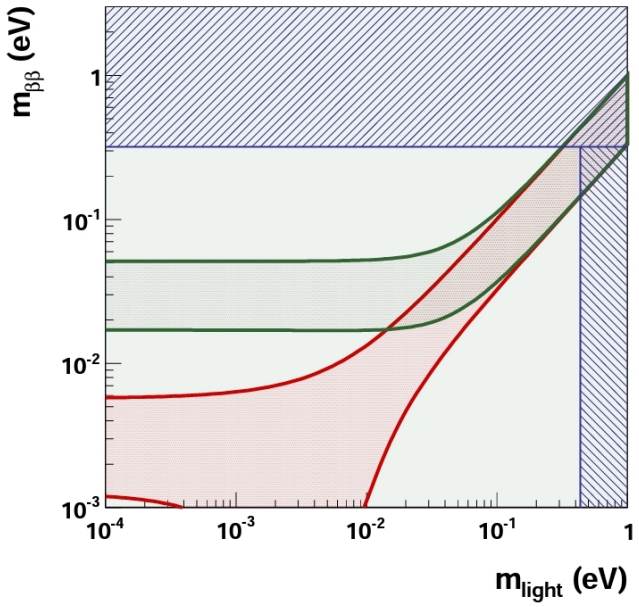

Figure 2.6: Values of the effective Majorana mass as a function of the lightest neutrino mass for the different mass ordering schemes [35]: The region bounded by the green and red lines represent the allowed values of $\langle m_{ee} \rangle$ in the inverted and normal hierarchies, respectively. The vertical blue region to the right represents the region of m_{light} excluded from cosmological considerations, while the horizontal one comes from null results of $\beta\beta_{0\nu}$ searches.

Just to mention, we can express the rest of parameters of eq.(2.8) with $\ell = e, \mu$ like a explicit function of the mixing angles and neutrinos masses

such that

$$\begin{aligned}\langle m_{\mu\mu}\rangle =& U_{1\mu}^2 m_1 + U_{2\mu}^2 m_2 + U_{3\mu} m_3 \\ =& (c_{23}s_{12} + s_{23}c_{12}s_{13}e^{i\delta_{12}})^2 e^{2i\alpha_1} m_1 \\ &+ (c_{23}c_{12} - s_{23}s_{12}s_{13}e^{i\delta_{12}})^2 e^{2i\alpha_2} m_2 \\ &+ c_{13}^2 s_{23}^2 m_3,\end{aligned} \tag{2.18}$$

$$\begin{aligned}\langle m_{e\mu}\rangle =& \sum_j U_{ej} U_{\mu j} m_j \\ =& (c_{23}s_{12} + s_{23}c_{12}s_{13}e^{i\delta_{12}}) c_{13}c_{12} e^{2i\alpha_1} m_1 \\ &+ (c_{23}c_{12} - s_{23}s_{12}s_{13}e^{i\delta_{12}}) c_{13}s_{12} e^{2i\alpha_2} m_2 \\ &+ s_{12}c_{13}s_{23} e^{-2i\delta_{12}} m_3.\end{aligned} \tag{2.19}$$

Chapter 3

Double beta decays of hyperons

In this Chapter we present the main results of this thesis: the branching fractions for neutrinoless double beta decay of hyperons. For completeness we start summarizing the results for the branching ratios of the two-neutrino double beta decays of hyperons in the SM, which are the main source of background for neutrinoless decays. Then, we compute the maximum rates for $\beta\beta_{0\nu}$ decays using a one-loop model where the full momentum transfer-dependence of weak form factors is taken into account. These form factors serves as natural regulators for the, otherwise, divergent integrals. In our predictions we consider two interesting scenarios: 1) the contributions of only three light neutrinos species, and 2) the case of heavy Majorana states with masses around a few TeV's which are predicted in some low-scale seesaw models. Several improvements and extensions with respect to a previous work are presented.

In this thesis we refers as hyperons to the lowest lying SU(3) octet of spin-1/2 hadrons and are generically denoted as B (also called baryons). As is well known [19], hyperons can undergo non-leptonic, semileptonic (beta) and radiative weak decays as the dominant channels.

The Beijing Electron Spectrometer III (BESIII) collaboration has a great hyperon physic program, they are expecting to produce about 10^8 hyperons via J/Ψ and $\psi(2S)$ decays [10]. Moreover, BESIII is looking for different LNV channels of hyperons, recently they reported some interesting results about the upper limits of two transitions $B(\Sigma^- \to pe^-e^-) < 6.7 \times 10^{-5}$ [11] and $B(\Xi^- \to p\mu^-\mu^-) < 4 \times 10^{-8}$ [10].

3.1 $\beta\beta_{2\nu}$ decay of hyperons

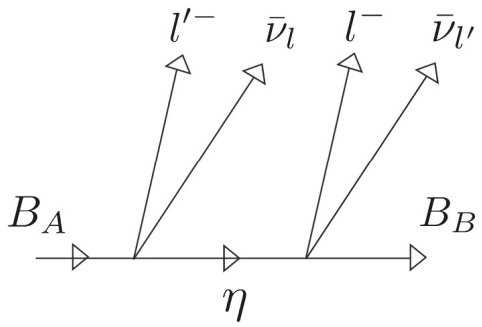

Figure 3.1: $\beta\beta_{2\nu}$ hyperon decay diagram in the local four-fermion approximation. $B_A = \Sigma^-$, Ξ^-, $B_B = \Sigma^+$, p, and ℓ, ℓ' are charged leptons (e, μ) of all the kinematically allowed channels (see table 3.1). Here η stands for the baryon intermediate state.

Transition		BR with all intermediate states	BR with Σ^0 intermediate state
Σ^-	$\to \Sigma^+ e^- e^- \bar{\nu}\bar{\nu}$	8.59×10^{-31}	8.59×10^{-31}
	$\to p e^- e^- \bar{\nu}\bar{\nu}$	1.02×10^{-3}	2.85×10^{-23}
	$\to p e^- \mu^- \bar{\nu}\bar{\nu}$	4.5×10^{-4}	1.23×10^{-23}
Ξ^-	$\to \Sigma^+ e^- e^- \bar{\nu}\bar{\nu}$	6.59×10^{-14}	5.57×10^{-25}
	$\to \Sigma^+ e^- \mu^- \bar{\nu}\bar{\nu}$	1.20×10^{-15}	6.78×10^{-27}
	$\to p e^- e^- \bar{\nu}\bar{\nu}$	4.68×10^{-7}	1.85×10^{-17}
	$\to p e^- \mu^- \bar{\nu}\bar{\nu}$	3.80×10^{-7}	8.00×10^{-18}
	$\to p \mu^- \mu^- \bar{\nu}\bar{\nu}$	5.59×10^{-8}	9.75×10^{-20}

Table 3.1: Branching ratios for $\beta\beta_{2\nu}$ of hyperons reported in Ref. [36]

The main source of background for $\beta\beta_{0\nu}$ hyperon decays comes from the $\beta\beta_{2\nu}$ $B_A \to B_B \ell^- \ell'^- \bar{\nu}_\ell \bar{\nu}_{\ell'}$, which are rare decays in the SM since they occurs at second order in the weak interactions as shown in fig. 3.1. The calculation of this kind of decays was first computed in [12,36]. In the first of these works the authors have estimated the BR using the decay chain illustrated in Fig. (3.1). The effective weak Hamiltonian for the $\Sigma^- \to \Sigma^+ e^- e^-$ process at each

interaction vertex is given by

$$H = \frac{G}{\sqrt{2}} J^{\mu} j_{\mu}, \tag{3.1}$$

where $G = G_F V_{ud}$ and the hadronic and leptonic currents are defined as

$$J^{\mu} = \bar{\psi}_u \gamma^{\mu}(1-\gamma^5)\psi_d, \quad j_{\mu} = \bar{\psi}_e \gamma_{\mu}(1-\gamma^5)\psi_{\nu} \ . \tag{3.2}$$

The decay amplitude can be written as follows

$$\begin{aligned} \mathcal{M}_{2\nu} &= [1 - P(e_1 e_2)][1 - P(\nu_1 \nu_2)] \\ &\sum_{\eta=\Sigma^0,\Lambda} \frac{\langle p_B; e_1 e_2 \nu_1 \nu_2 | H | \eta, Q; e_1 \nu_1 \rangle \langle \eta, Q; e_1 \nu_1 | H | p_A \rangle}{m_A - \epsilon_1 - \omega_1 - \epsilon_Q}, \end{aligned} \tag{3.3}$$

where $\epsilon_Q = \sqrt{Q^2 + m_\eta^2}$ is the energy of the intermediate neutral state, and ϵ_i, ω_i are the energies of the electrons and neutrinos, respectively. Using the weak form factors at zero momentum transfer (a very good approximation in this case), the authors of Ref. [12] have obtained the Branching ratio $\mathcal{B}(\Sigma^- \to \Sigma^+ e^- e^- \bar{\nu}\bar{\nu}) = 1.38 \times 10^{-30}$.

Meanwhile, in Ref. [36] they have estimated the branching fractions of the $\beta\beta_{2\nu}$ by assuming the decay chain $B_A \to \eta \ell^- \bar{\nu}_\ell \to B_B \ell^- \ell'^- \bar{\nu}_\ell \bar{\nu}_{\ell'}$. Taking the dominance of the on-shell intermediate states, which dominates by far the decay amplitude, one is led to following formula

$$\Gamma(B_A \to B_B \ell^- \ell'^- \bar{\nu}_\ell \bar{\nu}_{\ell'}) = \sum_{\eta} \Gamma(B_A \to \eta \ell^- \bar{\nu}_\ell) \times \mathcal{B}(\eta \to B_B \ell'^- \bar{\nu}_{\ell'}). \tag{3.4}$$

Their results for the branching fractions are reported in Table 3.1.

3.2 $\beta\beta_{0\nu}$ decay of hyperons

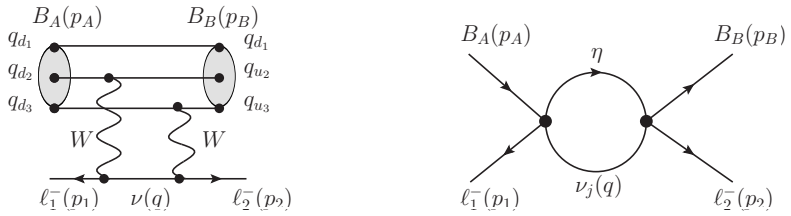

Figure 3.2: $\beta\beta_{0\nu}$ decay of hyperons in the presence of Majorana neutrinos. Diagram (a) represents the transition at the quark level. At low-energies, the transition can be represented by an effective one-loop mechanism, diagram (b).

$\Delta S = 0$	$\Delta S = 1$	$\Delta S = 2$
$\Sigma^- \to \Sigma^+ e^- e^-$	$\Sigma^- \to p e^- e^-$	$\Xi^- \to p e^- e^-$
	$\Sigma^- \to p^+ \mu^- \mu^-$	$\Xi^- \to p \mu^- \mu^-$
	$\Sigma^- \to p^+ \mu^- e^-$	$\Xi^- \to p \mu^- e^-$
	$\Xi^- \to \Sigma^+ e^- e^-$	
	$\Xi^- \to \Sigma^+ \mu^- e^-$	

Table 3.2: Different channels for $\beta\beta_{0\nu}$ hyperon decays.

Let us focus on the processes $B_A^- \to B_B^+ \ell_1^- \ell_2^-$ shown in fig. 3.2. If Majorana neutrinos are present $\beta\beta_{0\nu}$ hyperon decays may be induced at one-loop level by the effective diagram in Fig. 3.2. All the different channels can be classified according to their change on strangeness ΔS as is depicted in table 3.2, and, in general, the amplitude can be written as follows [1]:

$$i\mathcal{M} = -G^2 \sum_j m_{\nu_j} U_{\ell_1 j} U_{\ell_2 j} \sum_\eta \int \frac{d^d q}{(2\pi)^d} \frac{L^{\alpha\beta}(p_1, p_2)}{[q^2 - m_{\nu_j}^2]} \frac{h_{\alpha\beta}(p_A, p_B)}{[Q^2 - m_\eta^2]} - (\ell_1(p_1) \leftrightarrow \ell_2(p_2)) \,, \tag{3.5}$$

[1] Note that in eq. (3.5) we are considering the integration in $d = 4 - 2\epsilon$ ($\epsilon \to 0$) dimensions because our results are presented in terms of the Passarino-Veltman functions where dimensional regularization is used in order to isolate the UV divergences.

Transition	η	$f_{A\eta}$	$g_{A\eta}$	$f_{B\eta}$	$g_{A\eta}$
$\Sigma^- \to \Sigma^+$	Λ	0	0.656	0	0.656
	Σ^0	$\sqrt{2}$	0.655	$\sqrt{2}$	-0.656
$\Sigma^- \to p$	n	-1	0.341	1	1.267
	Σ^0	$\sqrt{2}$	0.655	$-1/\sqrt{2}$	0.241
	Λ	0	0.656	$-\sqrt{3/2}$	-0.895
$\Xi^- \to \Sigma^+$	Ξ^0	-1	0.341	1	1.267
	Σ^0	$1/\sqrt{2}$	0.896	$\sqrt{2}$	-0.655
	Λ	$\sqrt{3/2}$	0.239	0	0.656
$\Xi^- \to p$	Σ^0	$1/\sqrt{2}$	0.896	$-1/\sqrt{2}$	0.241
	Λ	$\sqrt{3/2}$	0.239	$-\sqrt{3/2}$	-0.895

Table 3.3: Vector and axial form factors for weak hyperon decays at zero momentum transfer. Here η stands for the baryon intermediate state, and the subscript A (B) represents the initial (final) baryon taken from [36] [37].

where $Q = p_A - p_1 - q$ the momentum carried by the intermediate state η, $U_{\ell_1 j}$ and $U_{\ell_2 j}$ are the mixing matrix elements connecting flavor and mass neutrino eigenstates, $\ell_1 \leftrightarrow \ell_2$ stands for an identical diagram contribution when the external charged lepton are identical and we have defined

$$L^{\alpha\beta} \equiv \bar{u}(p_2)\gamma^\alpha(1-\gamma_5)\gamma^\beta v(p_1), \tag{3.6}$$

$$h_{\alpha\beta} \equiv \bar{u}(p_B)\gamma_\alpha \left(f_{B\eta}(q''^2) + g_{B\eta}(q''^2)\gamma_5\right)(\not{Q} + m_\eta)\gamma_\beta \times \left(f_{A\eta}(q'^2) + g_{A\eta}(q'^2)\gamma_5\right) u(p_A), \tag{3.7}$$

$$G^2 \equiv G_F^2 \begin{cases} V_{ud}^2 & \text{for} \quad \Delta S = 0, \\ V_{ud}V_{us} & \text{for} \quad \Delta S = 1, \\ V_{us}^2 & \text{for} \quad \Delta S = 2, \end{cases} \tag{3.8}$$

with G_F the Fermi constant. Note also that the transition factors $f_{(A,B)\eta}$ and $g_{(A,B)\eta}$ parameterize the vector and axial currents, respectively, and they will depend on the squared momentum transfer [2]. At zero momentum transfer their values have been reported by different groups [8, 37] with good agreement among them (see table 3.3).

Notice that the amplitude can be rearranged conveniently distributing the factors in eq. (3.7), thus the hadronic part $h_{\alpha\beta}$ can be written as follows

$$h_{\alpha\beta} = \bar{u}(p_B)\gamma_\alpha \left[\left(\kappa_{v_+} + \kappa_{a_+}\gamma_5\right)\not{Q} + m_\eta\left(\kappa_{v_-} - \kappa_{a_-}\gamma_5\right)\right]\gamma_\beta u(p_A), \tag{3.9}$$

[2]Specifically $f_{A\eta}$ and $g_{A\eta}$ depend on $q''^2 = (p_2 - q)^2$, whereas $f_{B\eta}$ and $g_{B\eta}$ depend on $q'^2 = (p_1 + q)^2$.

with the definitions

$$\kappa_{v_\pm}(q^2) \equiv f_{A\eta}(q'^2) f_{B\eta}(q''^2) \pm g_{A\eta}(q'^2) g_{B\eta}(q''^2), \tag{3.10}$$
$$\kappa_{a_\pm}(q^2) \equiv f_{B\eta}(q''^2) g_{A\eta}(q'^2) \pm g_{B\eta}(q''^2) f_{A\eta}(q'^2). \tag{3.11}$$

Defining

$$H^j_{\alpha\beta}(p_1, p_2) \equiv \sum_\eta \int \frac{d^d q}{(2\pi)^d} \frac{h_{\alpha\beta}}{[q^2 - m^2_{\nu_j}][Q^2 - m^2_\eta]}, \tag{3.12}$$

it turns clear that, after the loop integration, the hadronic part can be written in the following form

$$\begin{aligned} H^j_{\alpha\beta}(p_1, p_2) = \sum_\eta \bar{u}(p_B)\gamma_\alpha \Big[&\left(C^{\eta j}_{v_0} + C^{\eta j}_{a_0}\gamma_5\right) m_{\eta j} + \left(C^{\eta j}_{v_1} + C^{\eta j}_{a_1}\gamma_5\right) \not{p}_1 \\ &+ \left(C^{\eta j}_{v_2} + C^{\eta j}_{a_2}\gamma_5\right) \not{p}_2 + \left(C^{\eta j}_{v_A} + C^{\eta j}_{a_A}\gamma_5\right) \not{p}_A \Big] \gamma_\beta u(p_A), \end{aligned} \tag{3.13}$$

where the factors $C_{v_{\{0,1,2,A\}}}$ and $C_{a_{\{0,1,2,A\}}}$ capture all the effects of the strong interactions relevant in the loop computation. Thus the amplitude (3.5) can be expressed simply as

$$i\mathcal{M} = -G^2 \sum_j m_{\nu_j} U_{\ell_1 j} U_{\ell_2 j} L^{\alpha\beta}(p_1, p_2) H^j_{\alpha\beta}(p_1, p_2) - (\ell_1 \leftrightarrow \ell_2). \tag{3.14}$$

3.2.1 Constant form factors approximation

In the approximation considered in ref. [12] where $f_{\{A,B\}_\eta}$ and $g_{\{A,B\}_\eta}$ are assumed constants in eqs. (3.10) and (3.11), we have that the relevant form factors in eq. (3.13) are given by

$$C^{\eta j}_{v_0} = i\frac{\kappa_{v_-}(0)}{16\pi^2} B_0(t, m^2_{\nu_j}, m^2_\eta), \tag{3.15}$$
$$C^{\eta j}_{v_A} = -C^{\eta j}_{v_1} = i\frac{\kappa_{v_+}(0)}{16\pi^2} \left[B_0(t, m^2_{\nu_j}, m^2_\eta) + B_1(t, m^2_{\nu_j}, m^2_\eta) \right], \tag{3.16}$$
$$C^{\eta j}_{v_2} = 0, \tag{3.17}$$

and

$$C^{\eta j}_{a_0} = -i\frac{\kappa_{a_-}(0)}{16\pi^2} B_0(t, m^2_{\nu_j}, m^2_\eta), \tag{3.18}$$
$$C^{\eta j}_{a_A} = -C^{\eta j}_{a_1} = i\frac{\kappa_{v_+}(0)}{16\pi^2} \left[B_0(t, m^2_{\nu_j}, m^2_\eta) + B_1(t, m^2_{\nu_j}, m^2_\eta) \right], \tag{3.19}$$
$$C^{\eta j}_{a_2} = 0, \tag{3.20}$$

where $t \equiv (p_A - p_1)^2$. Analytical expressions from the above Passarino-Veltman functions can be derived straightforwardly using Feynman parametrization. The important point to highlight here is that both B_0 and B_1 functions are ultraviolet divergent (further details are presented in the Appendix). Using dimensional regularization ($d = 4 - 2\epsilon$) the divergences can be isolated poles in ϵ (see table 3.4).

Function	Div part
B_0	Δ
B_1	$\Delta/2$

Table 3.4: Divergent part of the B_0 and B_1 functions, where $\Delta = \frac{1}{\epsilon} - \gamma_E + \log 4\pi$ and γ_E is the Euler-Mascheroni constant.

In Fig. (3.3) we plotted the behavior of eqs. (3.15) and (3.16) as a function of the neutrino mass (m_{ν_j}) for the $\Sigma^- \to pe^-e^-$ transition and only considering the intermediate state $\eta = n$ [3]. Also, we have fixed the Mandelstam variable t in its maximum value allowed by phase-space, according to the eq. (C.29). This plot lets us compare the evaluation of the loop integrals in two different approaches. The solid lines represent the finite part of the Passarino-Veltman functions using dimensional regularization, whereas the dashed lines stand for the cut-off approximation employed in [36] where the neutrino masses were neglected. We can see that in both schemes the dominant contribution comes from $C_{v_0}^{\eta j}$, being around a factor 10 larger than the rest of the coefficients. These conclusions can be extrapolated to the rest of transitions in Table 3.2.

3.2.2 q^2-dependence of the form factors

We have seen that in the constant form factor approximation the resulting loop integrals are logarithmically divergent. This bad behavior can be cured by taking into account the q^2-dependence of the weak hyperon form factors [4]. Measurements of the form factors in electron-nucleon scattering shows that they can be well described by the pole-type at non-zero but finite momentum transfer values. In a similar way as the mesons, one may expect that the form factors behave as $1/q^2$ in the asymptotic large q^2 regime [40]. Our original

[3] The COLLIER library [38] was used for the numerical evaluation of the Passarino-Veltman functions.

[4] This treatment has also been employed in the computation of the long-distance contributions to $K^+ \to \pi^+ \bar{\nu}\nu$ in [39].

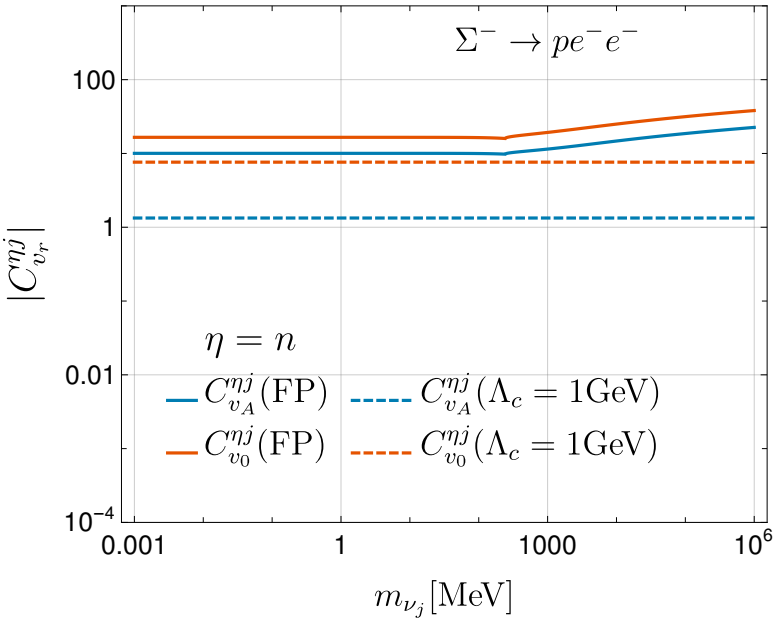

Figure 3.3: $C_{v_i}^{\eta j}$ dependence on m_{ν_j} for the constant form factor approximation.

idea was to use a form factor that extrapolates the behavior between the low and high q^2 momentum tranfers regimes. Unfortunately, to the best of our knowledge, no calculation have been reported so far regarding the behavior of the nucleon form factors at large momentum transfer (private communication with S. J. Brodsky). It has been found [8] that the measured form factors can be described by a dipole approximation. We find that a single pole approximation with rescaled pole masses is sufficient to approximate the dipole formula for low and intermediate momentum transfer values and make easier the loop integrations. Therefore, we will assume the following q^2 dependence of the form factors

$$f_i(q^2) = f_i(0)\left(1 - \frac{q^2}{m_{f_i}^2}\right)^{-1}, \quad g_i(q^2) = g_i(0)\left(1 - \frac{q^2}{m_{g_i}^2}\right)^{-1}, \tag{3.21}$$

where the rescaled pole masses are given by

$$\begin{aligned} m_{f_i} &= 0.84/\sqrt{2}\ (0.97/\sqrt{2})\,\text{GeV}, \\ m_{g_i} &= 1.08/\sqrt{2}\ (1.25/\sqrt{2})\,\text{GeV}, \end{aligned} \tag{3.22}$$

and $f_i(0)$ and $g_i(0)$ represent the vector and axial factors at zero momentum transfer (see table 3.3). The pole masses m_{f_i} and m_{g_i} corresponds to the

vectors and axial-vector strangeness-conserving form factors (pole maases corresponding to strangeness-changing are given within parentheses).

Under this approximation we have found that the relevant C_v form factors in eq. (3.9) are given by:

$$C_{v_0}^{\eta j} = \frac{i}{16\pi^2}\Big\{ f_{A_\eta}(0) f_{B_\eta}(0) m_{f_A}^2 m_{f_B}^2 D_0(m_{f_A}, m_{f_B}) - g_{A_\eta}(0) g_{B_\eta}(0) m_{g_A}^2 m_{g_B}^2 D_0(m_{g_A}, m_{g_B}) \Big\}, \tag{3.23}$$

$$C_{v_A}^{\eta j} = \frac{i}{16\pi^2}\Big\{ f_{A_\eta}(0) f_{B_\eta}(0) m_{f_A}^2 m_{f_B}^2 \left[D_1(m_{f_A}, m_{f_B}) + D_0(m_{f_A}, m_{f_B})\right] + g_{A_\eta}(0) g_{B_\eta}(0) m_{g_A}^2 m_{g_B}^2 \left[D_1(m_{g_A}, m_{g_B}) + D_0(m_{g_A}, m_{g_B})\right] \Big\} \tag{3.24}$$

$$C_{v_1}^{\eta j} = \frac{i}{16\pi^2}\Big\{ f_{A_\eta}(0) f_{B_\eta}(0) m_{f_A}^2 m_{f_B}^2 \times \left[-D_2(m_{f_A}, m_{f_B}) - D_1(m_{f_A}, m_{f_B}) - D_0(m_{f_A}, m_{f_B})\right] + g_{A_\eta}(0) g_{B_\eta}(0) m_{g_A}^2 m_{g_B}^2 \times \left[-D_2(m_{g_A}, m_{g_B}) - D_1(m_{g_A}, m_{g_B}) - D_0(m_{g_A}, m_{g_B})\right] \Big\}, \tag{3.25}$$

$$C_{v_2}^{\eta j} = \frac{i}{16\pi^2}\Big\{ f_{A_\eta}(0) f_{B_\eta}(0) m_{f_A}^2 m_{f_B}^2 D_3(m_{f_A}, m_{f_B}) + g_{A_\eta}(0) g_{B_\eta}(0) m_{g_A}^2 m_{g_B}^2 D_3(m_{g_A}, m_{g_B}) \Big\}, \tag{3.26}$$

with the arguments of the Passarino-Veltman functions given by

$$D_{\{0,1,2,3\}}(m_X,\, m_Y) \equiv D_{\{0,1,2,3\}}\left(t, m_A^2, s, m_2^2, m_1^2, m_B^2, m_{\nu_j}, m_\eta, m_X, m_Y\right), \tag{3.27}$$

and we have introduced the Maldestam variables $u \equiv (p_A - p_2)^2$, $t \equiv (p_A - p_1)^2$ and $s+t+u = m_A^2 + m_B^2 + m_1^2 + m_2^2$. As far the C_a factors are concerned, they can be obtained straightforwardly from the above expressions considering the following replacements

$$C_{a_0}^{\eta j} \equiv -C_{v_0}^{\eta}\left(f_{A\eta} \leftrightarrow g_{A\eta},\ m_{f_A} \leftrightarrow m_{g_A}\right), \tag{3.28}$$

$$C_{\{a_1,\, a_2,\, a_A\}}^{\eta j} \equiv C_{\{v_1,\, v_2,\, v_A\}}^{\eta}\left(f_{A\eta} \leftrightarrow g_{A\eta},\ m_{f_A} \leftrightarrow m_{g_A}\right). \tag{3.29}$$

3.2.3 Numerical analysis

Notice that the relevant vector and axial factors appearing in the amplitude (3.14) are

$$C_{v_r}^{\eta} \equiv \sum_j m_{\nu_j} U_{\ell_1 j} U_{\ell_2 j} C_{v_r}^{\eta j} \quad \text{with} \quad r = 0, 1, 2, A, \tag{3.30}$$

$$C_{a_r}^{\eta} \equiv \sum_j m_{\nu_j} U_{\ell_1 j} U_{\ell_2 j} C_{a_r}^{\eta j} \quad \text{with} \quad r = 0, 1, 2, A. \tag{3.31}$$

For now, let us focus in the dependence of (m_{ν_j}) for the one-loop functions

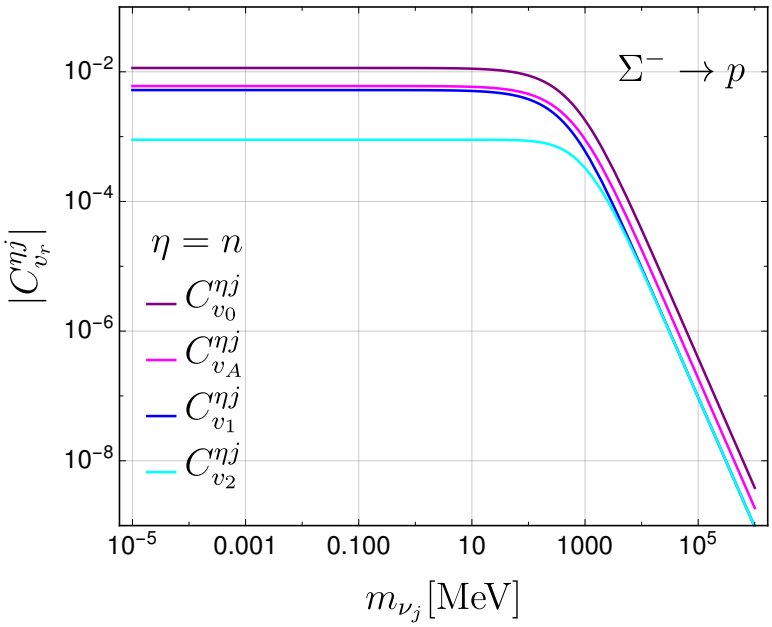

Figure 3.4: $C_{v_r}^{nj}$ form factors for the $\Sigma^- \to p$ transition as function of the neutrino mass m_ν assuming a pole-type dependence for the form factors.

$C_{v_r}^{\eta j}$ functions. In fig. 3.4, we illustrate their behavior in the pole-type approximation as a function of the neutrino mass m_{ν_j} for the $\Sigma^- \to p$ transition (very similar plots are obtained for the axial factors and also for all the different intermediate η baryons). For illustrative purposes, we have considered in Fig. 3.4 the maximal allowed values for the Mandelstam variables t and u [5].

[5]We verified that the masses of the external charged leptons (m_e, m_μ) are not relevant in the behavior of the loop function, even for the μ lepton.

Contrary to references [12, 36], we have kept finite masses for the neutrinos, which, as we will see, allows us to consider also the case of neutrinos with masses around few TeV.

We have checked that in all the different channels the dominant contributions come from the C_{v_0} and C_{a_0} factors as long as they are not zero. From this plot it turns out clear that for small neutrino masses ($\lesssim 100$ MeV) all the form factors are almost insensitive to the growth of the neutrino mass. Therefore, if all the masses of the neutrino states are in this interval, the approximation where $m_{\nu_j} = 0$ in the argument of the Passarino-Veltman functions in eq. (3.27) is well justified. In other words, the relevant factors in eqs. (3.30) and (3.31) can be approximated by

$$C^{\eta}_{v_r} = \langle m_{\ell_1\ell_2}\rangle\, C^{\eta 0}_{v_r}, \tag{3.32}$$

$$C^{\eta}_{a_r} = \langle m_{\ell_1\ell_2}\rangle\, C^{\eta 0}_{a_r}, \tag{3.33}$$

where $C^{\eta 0}_{v_r}$ and $C^{\eta 0}_{a_r}$ corresponds to the evaluation of eqs. (3.23) and (3.26) at $m_{\nu_j} = 0$, letting us write the effective Majorana mass as a common factor in eq. (3.14). In particular, let's call *scenario (a)* to the case of three light Majorana neutrinos parameterized by the current limits of the effective Majorana masses [6]:

$$\langle m_{ee}\rangle = 0.36\,\text{eV}, \quad \langle m_{e\mu}\rangle = 17\,\text{MeV}, \quad \langle m_{\mu\mu}\rangle = 290\,\text{MeV}. \tag{3.34}$$

Moreover, note that the one-loop functions described in eq. (3.27) can be also applied for heavy neutrino masses, then it is also interesting to study the effects of hypothetical heavy Majorana neutrinos with masses around a few TeV predicted by several extensions to the SM. In particular, it is well known that the so-called low-scale seesaw models allow the presence of heavy Majorana states with arbitrary masses and then unsupressed heavy-light mixings, constrained only by perturbative and the experimental limits.

Let's call *scenario (b)* to the contributions to $\beta\beta_{0\nu}$ decays of hyperons due to heavy Majorana masses in low-scale seesaw models. In order to quantify these effects, we will consider the minimal parametrization presented in reference [41]. Here the neutrino sector consists of 5 Majorana fields ($\chi_i = \chi_{L_i} + \chi^c_{L_i}$) and the charged weak lepton current relevant for our computation is described by the lagrangian:

$$\mathcal{L}^{\pm}_{W} = -\frac{g}{2\sqrt{2}} W^{-}_{\mu} \sum_{i=1}^{3}\sum_{j=1}^{5} B_{ij}\bar{\ell}_i\gamma^{\mu}(1-\gamma_5)\chi_j + \text{h.c.}, \tag{3.35}$$

[6] These numbers have been taken from [35].

where B is a 3×5 rectangular matrix

$$B_{ij} = \sum_{k=1}^{3} \delta_{ik} U^{\nu}_{kj}, \tag{3.36}$$

and U is the matrix that diagonalizes the neutrino mass matrix [7].

The relevant point here is that all the genuine effects of LNV can be parametrized in terms of the mass splitting ($r = m^2_{N_2}/m^2_{N_1}$) between the two heavy neutrinos $N_{1,2} \equiv \chi_{4,5}$.

The elements of the matrix B involving the heavy states in eq. (3.36) can be expressed in terms of the heavy-light mixings (s_{ν_k} with $k = e, \mu, \tau$) and the r parameter as follows:

$$B_{kN_1} = -i \frac{r^{1/4}}{\sqrt{1 + r^{1/2}}} s_{\nu_k}, \quad B_{kN_2} = \frac{1}{\sqrt{1 + r^{1/2}}} s_{\nu_k}. \tag{3.37}$$

One important point to remark for our analysis is that, in a realistic low-seesaw scenario, besides the direct and indirect constraints on s_{ν_k} we also have to consider the perturbative unitarity limit. In this model, that condition is translated in the relation

$$m_{N_1} r^{1/4} < \frac{\sqrt{2}\pi v}{\max\{s_{\nu_i}\}}. \tag{3.38}$$

Because we are interested in the estimate the maximum rate of the $\beta\beta_{0\nu}$ hyperon decays we will focus on new states with masses around a few TeV where the directs limits on the heavy-light mixings are less restrictive [8]. Then we only considered the mass-independent indirect limits on the heavy-light mixings coming from the current global fits to electroweak precision observables [44, 45]

$$s_{\nu_e} < 0.050, \quad s_{\nu_\mu} < 0.021, \quad s_{\nu_\tau} < 0.075. \tag{3.39}$$

Assuming the maximal values of (3.39) in eq. (3.38) implies that $m_{N_1} r^{1/4} < 8.2\,\text{TeV}$. In Fig. 3.5 we illustrate the behavior of the dominant $C^{\eta}_{v_0}$ factor as function of r for representative values of m_{N_1} and assuming the current indirect limits of the heavy-light mixing angles in (3.39) (similar plots can be obtained for the rest of vectorial and axial factors). Here we can see that if both states N_1 and N_2 form a heavy Dirac neutrino singlet (r=1)

[7] For more details of this parametrization we refer the reader to [41].

[8] Limits for the heavy-light mixings of new sterile neutrino states with masses $m_N \lesssim M_Z$ can be found in [42, 43].

then the lepton number is conserved, implying that the amplitude of the process goes to zero. On the other hand, this plot shows a comparison of $C_{v_0}^{\eta}$ in both mentioned scenarios. In the second of them, $C_{v_0}^{\eta}$ for $\Sigma^- \to pe^-e^-$ transition are increased until $\sim 10^6$ times compared with the same factor in the *scenario (a)* due to the restrictive limits of the effective Majorana mass $\langle m_{ee}\rangle$. In contrast, the $C_{v_0}^{\eta}$ factor involved in the transition $\Sigma^- \to pe^-\mu^-$ in the *scenario (b)* is below than *scenario (a)* where the limits in the effective Majorana mass $\langle m_{m\mu}\rangle$ are less restrictive. The results on the Branching fraction for the different LNV hyperon decay channel in both scenarios are reported in Table 3.5.

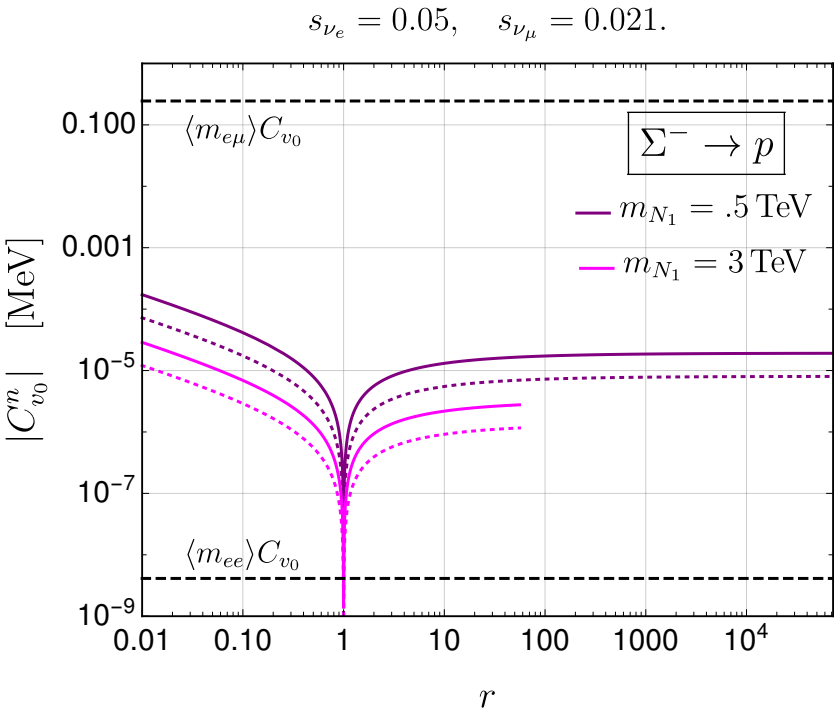

Figure 3.5: $C_{v_0}^{n}$ as a funtion of the ratio $r = m_{N_2}^2/m_{N_1}^2$, showing the effects of two non-degenerate heavy Majorana neutrinos in a low-scale seesaw model for two different processes $\Sigma^- \to pe^-e^-$ (solid lines) and $\Sigma^- \to pe^-\mu^-$ (dotted lines). The lines stop in the perturbative limits according to eq. (3.38).

Transition	Branching Ratio	Branching Ratio
	Scenario (a)	Scenario (b)
$\Sigma^- \to \Sigma^+ ee$	6.1×10^{-40}	2.9×10^{-31}
$\Sigma^- \to pee$	8.3×10^{-33}	3.5×10^{-24}
$\Sigma^- \to p\mu\mu$	5.0×10^{-16}	9.7×10^{-27}
$\Sigma^- \to p\mu e$	2.3×10^{-18}	6.9×10^{-26}
$\Xi \to \Sigma^+ ee$	7.9×10^{-35}	3.0×10^{-26}
$\Xi \to \Sigma^+ \mu e$	8.8×10^{-22}	2.4×10^{-29}
$\Xi \to pee$	2.7×10^{-34}	2.0×10^{-25}
$\Xi \to p\mu\mu$	7.4×10^{-16}	2.7×10^{-27}
$\Xi \to p\mu e$	1.2×10^{-19}	6.1×10^{-27}

Table 3.5: Branching ratios for $\Delta L = 2$ Hyperon decays. For the scenario (a) we are considered the maximum values of the effective Majorana masses given by eq. (3.34). Whereas for the scenario (b) we had considering the representative values $m_{N_1} = 1$ TeV and $r = 0.01$, and the limits on the heavy-light mixings given by (3.39).

Conclusions

In this work, we studied the $\beta\beta_{0\nu}$ decays of hyperons arising from an effective one loop mechanism with baryons and Majorana neutrinos as intermediate states. Our results improve previous estimates reported in [12,36]. As a first improvement, we have considered in the loop integrals a single-pole structure for the momentum dependence of the intermediate hadronic form factors, which is based in electron-nucleon scattering experiments. The inclusion of form factors cures the UV divergent behavior appearing in [36] and leads us to more reliable estimates of the branching ratios. We report the maximum rates for all the nine possible different channels in two interesting scenarios. First, we considered the scenario of three light Majorana neutrinos exchange taking into account the current limits for the effective Majorana masses. In this case, we have found that the rates are $\sim 10^{-3}$ smaller than previous calculations [12, 36].

Furthermore, since we have not considered any additional approximation, our results are valid for any value of the neutrino mass. Therefore, unlike [36] we also explored the genuine effects of the heavy Majorana masses ($\sim$ TeV) in a low-scale seesaw scenario. In this case, we considered the minimal parametrization proposed in ref. [41] that incorporates five Majorana neutrinos (three active massless and two heavy and sterile) where the LNV effects are encoded in the mass splitting of the two heavy states. In this alternative scenario, we considered allowed values for the mass of the heavy states consistent with the current limits for the heavy-light mixing angles and the perturbative unitarity condition.

We conclude that, in both scenarios considered in this thesis, the observation of $\beta\beta_{0\nu}$ decays of hyperons are far away from the sensitivity of current experiments. However, forthcoming results from searches at the BESIII experiment together with our calculations, will be able to provide direct constraints on the effective Majorana masses of μe and $\mu\mu$ channels that are competititve with other searches. Of course, any positive signal of LNV in hyperon decays can not be attributed to the Majorana neutrinos scenarios considered in this thesis work.

Appendix A

Feynman rules for Majorana fermions

In this appendix, we present the Feynman rules for Majorana fermions, more details and the explicit derivation of the rules can be found in [46]. We consider the most general interaction between two fermions, either Dirac (Ψ) or Majorana (λ) fields with any scalar or vector field (Φ). The Dirac structures $\Gamma_i = 1, \gamma_5, \gamma_\mu, \gamma_\mu\gamma_5, \sigma_{\mu\nu}$ transform under the charge conjugate operator as follows

$$\Gamma_i' = \mathbf{C}\Gamma_i^T\mathbf{C}^{-1} = \eta_i\Gamma_i, \tag{A.1}$$

with

$$\eta_i = \begin{cases} 1 & \text{for} \quad \Gamma_i = 1,\, i\gamma^5,\, \gamma^\mu\gamma^5 \\ -1 & \text{for} \quad \Gamma_i = \gamma^\mu\,, \sigma^{\mu\nu} \end{cases} . \tag{A.2}$$

For each diagram, we apply the following algorithmic rules:

1. Write all possible contributions to the amplitude for a given process.
2. The presence of Majorana fields indeterminate the direction of the fermionic chain, therefore, it should be chosen an arbitrary orientation of the flow, for now we denote it with brown arrows.
3. Insert the appropriate analytic expression given in figs. A.1-A.3 for every element in the diagram, starting in an external leg an proceeding opposite to the chosen orientation.
4. Multiply by a factor (-1) for every closed loop.
5. Multiply by the permutation parity of the spinors in the obtained analytical expression with respect to some reference order.

Notice that the above rules must be independent of the direction of the chosen flow [46].

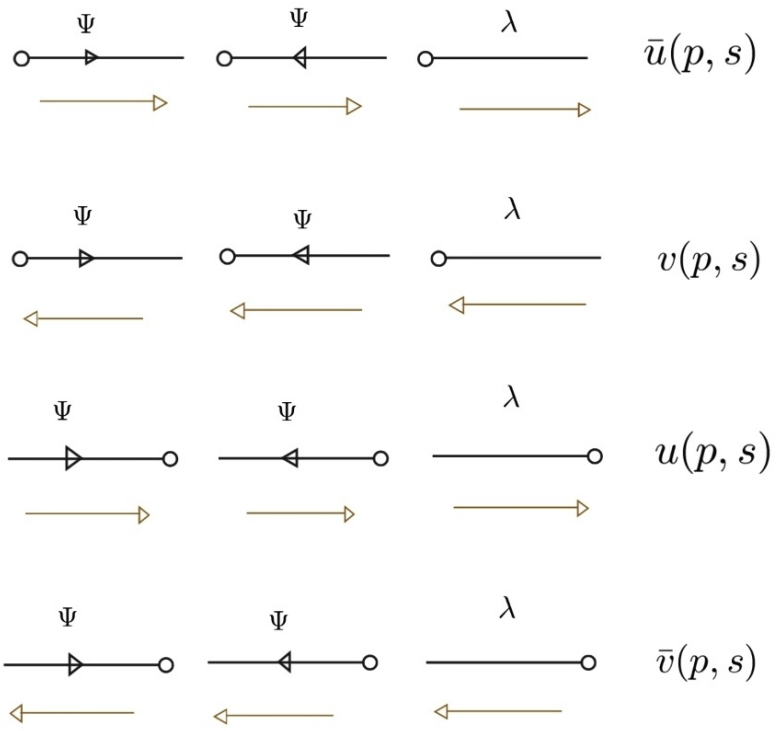

Figure A.1: Feynman rules for external fermion lines fixing fermionic flow (brown arrows).

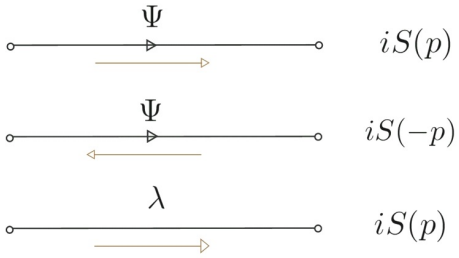

Figure A.2: Feynman rules for fermionic propagator for fixing fermionic flow (brown arrows), where $s(p) = i(\not{p} - m)^{-1}$.

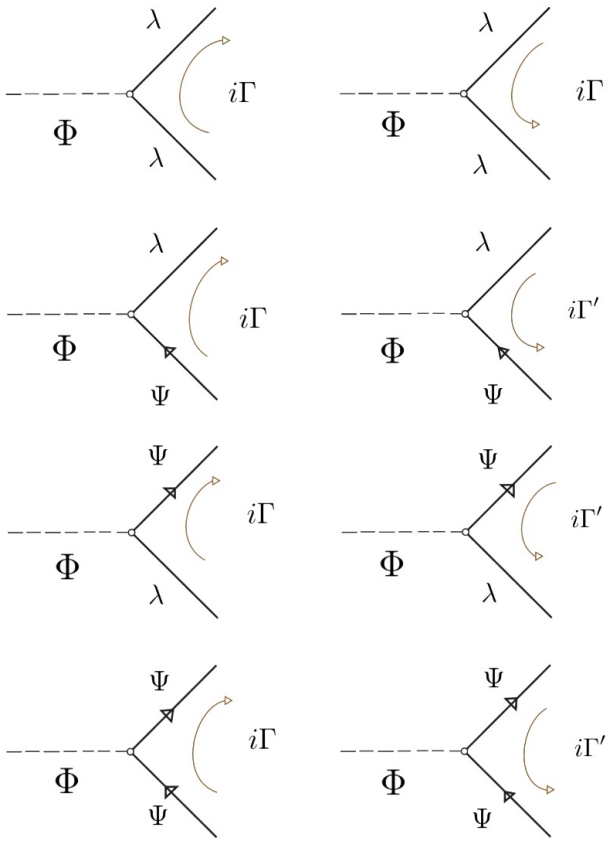

Figure A.3: Vertex Feynman rules for a fixing fermionic flow (brown arrows).

Appendix B

One loop integrals

In this appendix we give a brief summary and relevant formulas related to technical aspects of one loop computations. For a detailed explanation of this topic we refer the readers to [47].

B.1 Feynman parameters

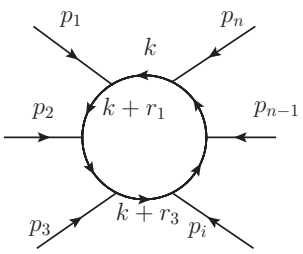

Figure B.1: Generic loop diagram and convention for the momentum.

In general, a one loop integral will take the form:

$$T_n^{\mu_1\mu_2\ldots\mu_p} = \int \frac{d^dk}{(2\pi)^d} \frac{N(k)}{A_1A_2\ldots A_n}, \tag{B.1}$$

where k represent the undetermined momentum inside the loop and the A_i factors are defined as

$$A_i = (k + r_i)^2 - m_i + i\epsilon, \tag{B.2}$$

every r_n is related to external momentum according to the Fig. B.1 such

that

$$r_i = \sum_{j=1}^{i} p_j, \quad (i = 1, 2, ..., n-1), \quad \text{and} \quad r_n = \sum_{k=1}^{n} p_k = 0. \tag{B.3}$$

In order to illustrate the Feynman parametrization method, we will compute the case where $N(k) = 1$ and $n = 2$. By combining the denominators it is possible to rewrite the product $1/A_1A_2$ as a common denominator using the Feynman parametrization given by

$$\frac{1}{A_1A_2} = \int_0^1 dx \frac{1}{(xA_1 + (1-x)A_2)^2}. \tag{B.4}$$

Thus, using $A_1 = (k+p_1)^2 - m_1^2 + i\epsilon_1$ and $A_2 = k^2 - m_2^2 + i\epsilon_2$ we have:

$$\begin{aligned} xA_1 + (1-x)A_2 &= x((k+p_1)^2 - m_1^2) + (1-x)(k^2 - m_2^2), \\ &= -m_2^2 - m_1^2 x + m_2^2 x + k.k + 2xk.p_1 + xp_1^2, \\ &= (k+l)^2 - M^2 + i\epsilon, \end{aligned} \tag{B.5}$$

using the on-shell mass condition for the external momentums and taking $l = xp_1$, $M^2 = (1-x)m_2^2 + x^2 m_1^2$ and $\epsilon = (1-x)\epsilon_2 + x\epsilon_1$. Then, we can write

$$\begin{aligned} I &= \int \frac{d^dk}{(2\pi)^d} \frac{1}{(k^2 - m_2^2 + i\epsilon_2)((k+p_1)^2 - m_1^2 + i\epsilon_1)} \\ &= \int_0^1 dx \int \frac{d^dk}{(2\pi)^d} \frac{1}{[(k+l)^2 - M^2 + i\epsilon]^2}. \end{aligned} \tag{B.6}$$

Now, taking $k' = k + l$ we can rearrange eq. (B.6) as follows

$$I = \int_0^1 dx \int \frac{d^dk'}{(2\pi)^d} \frac{1}{[k'^2 - M^2 + i\epsilon]^2}. \tag{B.7}$$

A general identity for eq. (B.4) can be found in ref. [48]

$$\frac{1}{A_1^{\alpha_2} A_2^{\alpha_2} ... A_n^{\alpha_n}} = \frac{\Gamma(\alpha)}{\Pi_i \Gamma(\alpha_i)} \int_0^1 dx_1 ... dx_n \delta\left(1 - \sum x_i\right) \frac{x_1^{\alpha_1 - 1} ... x_n^{\alpha_n - 1}}{[\sum_i x_i A_i]^\alpha}, \tag{B.8}$$

with $\alpha = \alpha_1 + ... + \alpha_n$.

B.2 Wick rotation

Notice that all the scalar loop-integrals

$$I_{r,m} = \int \frac{d^dk'}{(2\pi)^d} \frac{k'^{2r}}{(k'^2 - M^2 + i\epsilon)^m}, \tag{B.9}$$

can be rewritten by splitting the integral over k' such that

$$I_{r,m} = \int \frac{d^{d-1}k'}{(2\pi)^d} \int_{-\infty}^{\infty} \frac{dk'_0}{[k'^2_0 - (|\vec{k'}|^2 - M^2 - i\epsilon)]^2}. \tag{B.10}$$

Now, focusing first on the integral over k'_0, we proceed to evaluate it in an arbitrary path within the complex plane given by fig. B.2. As we know from complex analysis, the integration over both arcs is equal to zero when $R \to \infty$. Furthermore, the two poles of the integral are outside of the evaluation contour what lets us write, by the Cauchy's theorem, the follow identity

$$\int_{-\infty}^{\infty} f(k')dk'_0 = \int_{-i\infty}^{i\infty} f(k')dk'_0. \tag{B.11}$$

From the above equation we can change the integration from a real axis into

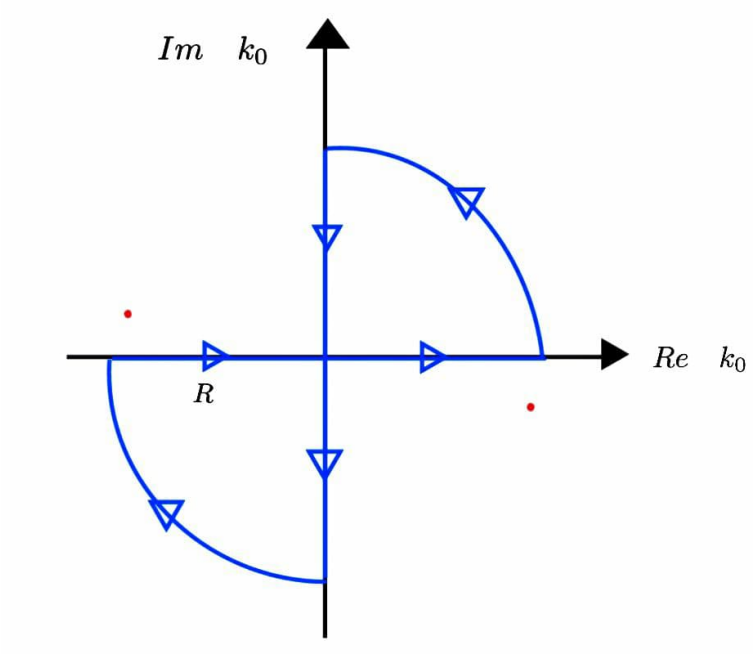

Figure B.2: Integration contour for k'_0. The red dots represent the two poles where $k'_0 \approx \pm\left(\sqrt{|\vec{k'}|^2 - M^2} - i\epsilon\right)$

an integral along the imaginary axis. Finally, if we use the change

$$k'_0 = ip_0, \quad \text{and} \quad \int_{-\infty}^{\infty} dk'_0 \to i\int_{-\infty}^{\infty} dp_0, \tag{B.12}$$

we can rewrite eq. (B.9) as follows

$$I_{r,m} = \frac{i(-1)^{r-m}}{(2\pi)^d} \int \frac{p^{2r} d^d p}{[p^2 + M^2]^m}, \tag{B.13}$$

where we defined $p^\mu = (p_0, \vec{k'})$ as an euclidean vector with norm $p^\mu p_\mu = |p|^2 = p^2 + |k'|^2$, this procedure is the so-called Wick rotation.

B.3 Dimensional Regularization

Notice that all the previous discussion has been considered for the integration over d dimensions. For $d = 4$ some of the loop integrals have an UV ($|p| \to \infty$) divergent behavior, which can be regulated by considering the limit $\epsilon \to 0$ in $d = 4 - 2\epsilon$. Lets illustrate this by considering eq. (B.13), here the hyper-volume element can be written as $d^d p = p^{d-1} dp d\Omega_d$. Then, the integration over the solid angle is given by

$$\int d\Omega_d = \frac{2\pi^{d/2}}{\Gamma(d/2)}, \tag{B.14}$$

where Γ is the special Gamma function, further details are found in [47]. Thus, the scalar one loop-integral in eq. (B.13) can be written as follows

$$I_{r,m} = \frac{i(-1)^{r-m}}{(2\pi)^{d/2}} \frac{2^{1-d/2}}{\Gamma(d/2)} \int_0^\infty \frac{p^{2r+d-1} dp}{[p^2 + M^2]^m}. \tag{B.15}$$

The solution of the above integral is well know in the literature and is given by

$$\int_0^\infty \frac{x^p dx}{(x^2 + M^2)^l} = \frac{M^{1+p-l} \Gamma(l - \frac{1+p}{2}) \Gamma(\frac{1+p}{2})}{2\Gamma(l)}, \tag{B.16}$$

as long as $\mathrm{Re}(M^2) > 0$ and $l > (1 + p)/2$. Taking $d = 4 - 2\epsilon$ it is easy to rearrange eq. (B.15) such that

$$I_{r,m} = \frac{i(-1)^{r-m}}{(2\pi)^{2-\epsilon/2}} \frac{2^{-1+\epsilon/2}}{\Gamma(2 - \frac{\epsilon}{2})} \frac{\Gamma(-2 + m - r + \frac{\epsilon}{2}) \Gamma(2 + r - \frac{\epsilon}{2})}{2\Gamma(m)} M^{-e+2r-2m+4}. \tag{B.17}$$

For example, the above general formula can match eq. (B.7) by taking $m = 2$ and $r = 0$ such that

$$I_{0,2} = \frac{i}{16\pi^2} \left(\frac{4\pi}{M^2} \right)^{\epsilon/2} \Gamma(\epsilon/2). \tag{B.18}$$

In the limit where $\epsilon \to 0$ the Γ function can be expanded by [47]

$$\Gamma(x) = \frac{1}{x} - \gamma_E + \mathcal{O}(x^2); \quad \text{with} \quad x \to 0, \tag{B.19}$$

where γ_E is the Euler-Mascheroni constant, meanwhile for the second term of the eq. (B.18) we can take an expansion such that

$$x^\epsilon = 1 + \epsilon \ln(x) + \mathcal{O}(\epsilon^3). \tag{B.20}$$

Finally, we can rearrange eq. (B.18) as follows

$$I_{0,2} = \frac{i}{16\pi^2}(\Delta - 2\ln(M) + \mathcal{O}(\epsilon)), \tag{B.21}$$

where Δ is defined as $\Delta \equiv \frac{2}{\epsilon} - \gamma_E + \log(4\pi)$. As we can see, the divergent part of the loop integral has been isolated as a pole $1/\epsilon$, this is the so-called dimensional regularization method.

In this appendix, we provide the expressions for the self-energy (two points loop functions) and box integrals (4 points functions) appearing in previous chapters [1].

- Self-energy integrals

$$\begin{aligned} I_{0,2} &= \frac{i}{16\pi^2}(\Delta_\epsilon - 2\ln M); \\ I_2^\mu &= \frac{i}{16\pi^2}(-\Delta_\epsilon + 2\ln M) l^\mu; \\ I_2^{\mu\nu} &= \frac{i}{32\pi^2}\left(M^2 g^{\mu\nu}(1 + \Delta_\epsilon - 2\ln M), +2(\Delta_\epsilon - 2\ln M) l^\mu l^\nu\right), \end{aligned} \tag{B.22}$$

with

$$l = x p_1; \quad M^2 = (1-x)m_2^2 + x^2 m_1^2. \tag{B.23}$$

- Box integrals

$$\begin{aligned} I_{0,4} &= \frac{i}{16\pi^2}\frac{1}{6M^4}; \\ I_4^\mu &= -\frac{i}{16\pi^2}\frac{1}{6M^4} l^\mu; \\ I_4^{\mu\nu} &= -\frac{i}{16\pi^2}\frac{1}{6M^4}\left(M^2 g^{\mu\nu} - 2 l^\mu l^\nu\right), \end{aligned} \tag{B.24}$$

[1] An extensive list for the expressions of the loop integrals with $m > 4$ can be found in [47].

with

$$\begin{aligned} l^{\mu} =&(x_1+x_2+x_3)p_1^{\mu}+x_2p_2^{\mu}+x_3p_2^{\mu}+x_3p_3^{\mu};\\ M^2 =&m_4^2-m_4^2x_1-m_1^2x_2-m_4^2x_2+m_2^2x_2^2-m_1^2x_3-m_2^2x_3-m_4^2x_3\\ &+2m_2^2x_2x_3+m_2^2x_3^2+m_3^2x_3^2+m_1^2(x_1+x_2+x_3)^2-2x_2p_1.p_2\\ &-2x_3p_1.p_2+2x_2(x_1+x_2+x_3)p_1.p_2+2x_3(x_1+x_2+x_3)p_1.p_2\\ &-2x_3p_1.p_3+2x_3(x_1+x_2+x_3)p_1.p_3-2x_3p_2.p_3+2x_2x_3p_2.p_3\\ &+2x_3^2p_2.p_3. \end{aligned} \tag{B.25}$$

We remark that the previous box-type integrals are free of UV divergences.

For completeness we discuss briefly the alternatively cut-off procedure used in [36] to regulate the ultraviolet divergences presented in the integrals of section 3.2.1. We illustrate this considering again eq. (B.15). For $r=0$, $m=2$ and taking $d=4$ directly we have that

$$I_{0,2}=\frac{i}{8\pi^2}\int_0^1 dx\int_0^{\infty}\frac{p^3dp}{[p^2+M^2]^2}. \tag{B.26}$$

As we can see, $I_{0,2}\sim\int dp/p$ has a logarithmic divergent behavior for $p\to\infty$. This ultraviolet behavior can be controlled by considering an upper bound (cut-off) for p [2], in such a case eq. (B.26) converts into

$$I_{0,2}=\frac{i}{8\pi^2}\int_0^1 dx\int_0^{\Lambda_c} dp\frac{p^3}{[p^2-M^2]^2}. \tag{B.27}$$

B.4 Passarino-Veltman functions

In general, the integration using Feynman parametrization becomes really tedious when we try to compute the integral over Feynman parameters in eqs. (B.22) and (B.25), but is a good way to identify and work with divergences. However, in order to compute numerical values of these integrals it is more convenient solving the problem using the scheme proposed by Passarino and Veltman in [49].

Scalar integral are really important because they generate tensorial loop integrals by taking derivatives of the first ones. Then using the typical no-

[2]Note that the cut-off procedure requires to assume physical considerations on the Λ_c scale. In reference [36], the value for Λ_c is related to the maximum distance length of the quarks inside the hyperons.

tation we name it as follows, redefining $r_0 \equiv r_n = 0$ and $m_0 \equiv m_n$

$$A_0(m_0) = \frac{(2\pi\mu)^\epsilon}{i\pi^2}\int d^dk \frac{1}{k^2 - m_0}; \tag{B.28}$$

$$B_0(r_{10}^2, m_0^2, m_1^2) = \frac{(2\pi\mu)^\epsilon}{i\pi^2}\int d^dk \prod_{i=0}^{1}\frac{1}{(k+r_i)^2 - m_i}; \tag{B.29}$$

$$C_0(r_{10}^2, r_{12}^2, r_{20}^2, m_0^2, m_1^2, m_2^2) = \frac{(2\pi\mu)^\epsilon}{i\pi^2}\int d^dk \prod_{i=0}^{2}\frac{1}{(k+r_i)^2 - m_i}; \tag{B.30}$$

$$D_0(r_{10}^2, ..., r_{13}^2, m_0^2, ..., m_3^2) = \frac{(2\pi\mu)^\epsilon}{i\pi^2}\int d^dk \prod_{i=0}^{3}\frac{1}{(k+r_i)^2 - m_i}. \tag{B.31}$$

Finally, as we have seen in previous sections we can compute these integrals as explicit function of the external momentum, then, this integral can be expressed in terms of reduced function, in particular we can write B^μ and D^μ as follows

$$B^\mu = r_1^\mu B_1; \tag{B.32}$$

$$D^\mu = \sum_{i=1}^{3} r_i^\mu D_i. \tag{B.33}$$

And their divergent parts can be written as:

$$\begin{aligned} \text{Div}[B_0(r_{10}^2, m_0^2, m_1^2)] &= m_0^2\Delta, \\ \text{Div}[B_1(r_{10}^2, m_0^2, m_1^2)] &= -\frac{1}{2}\Delta, \end{aligned} \tag{B.34}$$

$$\text{Div}[D_i] = 0. \tag{B.35}$$

Appendix C

Squared amplitude of $\beta\beta_{0\nu}$ decays

In this appendix we provide the expressions for the squared amplitude of the $\beta\beta_{0\nu}$ hyperon decay studied on chapter 3. As we have seen in eq. (3.14) there are two different contributions to the amplitude when external leptons are identical particles, these two diagrams are related to each other by the exchange $p_1 \leftrightarrow p_2$. Taking $\mathcal{M} = \mathcal{M}_1 - \mathcal{M}_2$, we define the individual contribution as:

$$\mathcal{M}_m = G^2 L^{(m)\alpha\beta} H^{(m)}_{\alpha\beta} \quad \text{with} \quad m = 1, 2, \tag{C.1}$$

where $L^{(m)\alpha\beta}$ and $H^{(m)}_{\alpha\beta}$ are defined according the eqs. (3.6) and (3.13) by

$$\begin{aligned} L^{(m)\alpha\beta} &\equiv L^{\alpha\beta}(p_m, p_{3-m}), \\ &= \bar{u}(p_{3-i})\gamma^\beta(1-\gamma^5)\gamma^\alpha v(p_i), \qquad \text{(C.2)} \\ H^{(m)}_{\alpha\beta} &\equiv \sum_j m_{\nu_j} U^2_{\ell j} H^j_{\alpha\beta} \qquad \text{(C.3)} \\ &= \sum_\eta \bar{u}(p_B)\gamma_\alpha \left[\left(C^{\eta(m)}_{v_0} + C^{\eta(m)}_{a_0}\gamma_5 \right) m_\eta + \left(C^{\eta(m)}_{v_1} + C^{\eta(m)}_{a_1}\gamma_5 \right) \not{p}_1 \right. \\ &+ \left. \left(C^{\eta(m)}_{v_2} + C^{\eta(m)}_{a_2}\gamma_5 \right) \not{p}_2 + \left(C^{\eta(m)}_{v_A} + C^{\eta(m)}_{a_A}\gamma_5 \right) \not{p}_A \right] \gamma_\beta u(p_A). \qquad \text{(C.4)} \end{aligned}$$

The vectorial factors in eq. (C.4) of the diagram 2 contribution can be written from the factors of diagram 1 with the following replacements

$$\begin{aligned} C^{\eta(2)}_{v_r} &= C^{\eta(1)}_{v_r}(u \leftrightarrow t), \quad \text{for} \quad v_r = v_0, v_A, \\ C^{\eta(2)}_{v_1} &= C^{\eta(1)}_{v_2}(u \leftrightarrow t), \\ C^{\eta(2)}_{v_2} &= C^{\eta(1)}_{v_1}(u \leftrightarrow t). \end{aligned} \tag{C.5}$$

Completely analogous expressions can be written for the axial factors. The notation in eq. (C.4) can be simplified by defining

$$c_{v_r}^{(m)} \equiv \sum_{\eta} C_{v_r}^{\eta(m)}, \quad c_{a_r}^{(m)} \equiv \sum_{\eta} C_{a_r}^{\eta(m)} \quad with \quad r = 1, 2, A \tag{C.6}$$

$$c_{v_0}^{(m)} \equiv \sum_{\eta} m_\eta C_{v_0}^{\eta(m)}, \quad c_{a_0}^{(m)} \equiv \sum_{\eta} C_{a_0}^{\eta(m)}, \tag{C.7}$$

what let us rewrite eq. (C.4) as follows

$$\begin{aligned} H_{\alpha\beta}^{(m)} = \bar{u}(p_A)\gamma_\beta \big\{ & (c_{v_A}^{(m)} + c_{a_A}^{(m)}\gamma^5)\not{p}_A + (c_{v_1}^{(m)} + c_{a_1}^{(m)}\gamma^5)\not{p}_1 \\ & + (c_{v_2}^{(m)} + c_{a_2}^{(m)}\gamma^5)\not{p}_2 + (c_{v_0}^{(m)} + c_{a_0}^{(m)}\gamma^5)\big\}\gamma_\alpha u(p_B). \end{aligned} \tag{C.8}$$

Taking the sum over all the polarization states of the external particles the total squared amplitude can be written as follows

$$|\overline{\mathcal{M}}|^2 = \frac{1}{2} \sum_{s_A, s_B, s_1, s_2} \left(|\mathcal{M}_1|^2 + |\mathcal{M}_2|^2 - 2Re(\mathcal{M}_1 \mathcal{M}_2^\dagger) \right), \tag{C.9}$$

where the first term in the above expression is given by

$$|\overline{\mathcal{M}_1}|^2 = \sum_s |\mathcal{M}_1|^2 = G^4 \sum_s B_{\mu\nu}^{(1)} (B_{\alpha\beta}^{(1)})^\dagger L^{(1)\mu\nu} (L^{(1)\alpha\beta})^\dagger. \tag{C.10}$$

Now, using the completeness relations:

$$\begin{aligned} \sum_s u(p)\bar{u}(p) &= \not{p} + m; \\ \sum_s v(p)\bar{v}(p) &= \not{p} - m, \end{aligned} \tag{C.11}$$

we have that

$$\sum_s L^{(1)\alpha\beta} (L^{(1)\mu\nu})^\dagger = \mathrm{Tr}[(\not{p}_2 + m_l)\gamma^\alpha(1-\gamma^5)\gamma^\beta(\not{p}_1 - m_l)\gamma^\nu(1+\gamma^5)\gamma^\mu], \tag{C.12}$$

and

$$\begin{aligned} \sum_s H_{\alpha\beta}^{(1)} (H_{\mu\nu}^{(1)})^\dagger = \mathrm{Tr}[(\not{p}_B + m_B)\gamma_\alpha (c_A^{(1)^\dagger}\not{p}_A + c_1^{(1)^\dagger}\not{p}_1 + c_2^{(1)^\dagger}\not{p}_2 + c_0^{(1)^\dagger}) \times \\ \gamma_\beta(\not{p}_A + m_A)\gamma_\nu (c_A^{(1)}\not{p}_A + c_1^{(1)}\not{p}_1 + c_2^{(1)}\not{p}_2 + c_0^{(1)})\gamma_\mu], \end{aligned} \tag{C.13}$$

where we write $c_r^{(m)} \equiv (c_{v_r}^{(m)} + c_{a_r}^{(m)}\gamma^5)$. The contribution of the diagram 2 in eq. (C.9) is obtained from eq. (C.10) just by changing the vectorial an axial $C_{a_r,v_r}^{\eta(1)}$ by the replacements in eq. (C.5).

In order to be able to use the completeness relations in the interference term of eq. (C.9), we have to use to do some intermediate steps. First, we have to consider the following relations

$$\begin{aligned} v(p,s) &= \mathbf{C}u^T(p,s), \\ u(p,s) &= \mathbf{C}v^T(p,s), \end{aligned} \tag{C.14}$$

and

$$\begin{aligned} \mathbf{C}\gamma_\mu^T\mathbf{C}^{-1} &= -\gamma_\mu, \\ \mathbf{C}(\gamma^5)^T\mathbf{C}^{-1} &= \gamma^5, \end{aligned} \tag{C.15}$$

then we can rearrange $L^{(2)\dagger}_{\mu\nu}$ as follows

$$\begin{aligned} (L^{(2)}_{\mu\nu})^\dagger &= \bar{v}(p_2)\gamma_\nu(1+\gamma^5)\gamma_\mu u(p_1) \\ &= u(p_1)^T\gamma_\mu^T(1+\gamma^5)^T\gamma_\nu^T\bar{v}(p_2)^T \\ &= u(p_1)^T\mathbf{C}^{-1}\mathbf{C}\gamma_\mu^T\mathbf{C}^{-1}\mathbf{C}(1+\gamma^5)^T\mathbf{C}^{-1}\mathbf{C}\gamma_\nu^T\mathbf{C}^{-1}\mathbf{C}\bar{v}(p_2)^T \\ &= -\bar{v}(p_1)\gamma_\mu(1+\gamma^5)\gamma_\nu u(p_2). \end{aligned} \tag{C.16}$$

Therefore, the interference term

$$\mathcal{M}_1\mathcal{M}_2^\dagger = G^4 H^{(1)}_{\mu\nu}(H^{(2)}_{\alpha\beta})^\dagger L^{(1)\mu\nu}(L^{(2)\alpha\beta})^\dagger, \tag{C.17}$$

can be written as follows

$$\sum_s L^{(1)\alpha\beta}(L^{(2)\mu\nu})^\dagger = -\mathrm{Tr}[(\not{p}_2 + m_l)\gamma^\alpha(1-\gamma^5)\gamma^\beta(\not{p}_1 - m_l)\gamma^\mu(1+\gamma^5)\gamma^\nu], \tag{C.18}$$

$$\begin{aligned} \sum_s H^{(1)}_{\alpha\beta}(H^{(2)}_{\mu\nu})^\dagger = \mathrm{Tr}[(\not{p}_B + m_B)\gamma_\alpha(c_A^{(2)^\dagger}\not{p}_A + c_1^{(2)^\dagger}\not{p}_1 + c_2^{(2)^\dagger}\not{p}_2 + c_0^{(2)^\dagger})\times \\ \gamma_\beta(\not{p}_A + m_A)\gamma_\nu(c_A^{(1)}\not{p}_A + c_2^{(1)}\not{p}_1 + c_1^{(1)}\not{p}_2 + c_0^{(1)})\gamma_\mu]. \end{aligned} \tag{C.19}$$

The inner products after take the trace can be written in terms of the well known Mandelstam variables for a $1 \to 3$ transition, they are given by:

$$s = (p_1+p_2)^2 = (p_A - p_B)^2, \tag{C.20}$$

$$t = (p_B+p_2)^2 = (p_A - p_1)^2, \tag{C.21}$$

$$u = (p_B+p_1)^2 = (p_A - p_2)^2, \tag{C.22}$$

where the relation $s+u+t=m_A^2+m_B^2+m_1^2+m_2^2$ is satisfied. In this way, we have that

$$\begin{aligned}
p_1\cdot p_2 &= \frac{1}{2}(m_A^2+m_B^2-u-t);\\
p_2\cdot p_B &= \frac{1}{2}(t-m_B^2-m_\ell^2);\\
p_A\cdot p_B &= \frac{1}{2}(u+t-2m_l^2);\\
p_1\cdot p_B &= \frac{1}{2}(u-m_B^2-m_\ell^2);\\
p_1\cdot p_A &= \frac{1}{2}(m_A^2+m_\ell^2-t);\\
p_2\cdot p_A &= \frac{1}{2}(m_A^2+m_\ell^2-u).
\end{aligned} \tag{C.23}$$

Finally, with the help of the FeynCalc package [50–52] to compute the traces in eqs. (C.12), (C.13), (C.18), and (C.19) we obtained that:

$$\begin{aligned}
|\overline{\mathcal{M}_1}|^2 &= -128G^4(m_A^2+m_B^2-t-u)(m_A(c_{v_1}^{(1)}m_l^2m_A+c_{v_2}^{(1)}m_l^2m_A\\
&-4c_{v_1}^{(1)}m_l^2m_B-c_{v_1}^{(1)}m_Au+4c_{v_2}^{(1)}m_Bu\\
&-4c_{v_2}^{(1)}m_l^2m_B-4c_{v_1}^{(1)}m_A^2m_B-4c_{v_2}^{(1)}m_A^2m_B+c_{v_1}^{(1)}m_Am_B^2+c_{v_2}^{(1)}m_Am_B^2\\
&-c_{v_2}^{(1)}m_At+4c_{v_1}^{(1)}m_Bt+2c_{v_0}^{(1)}(-2m_l^2+2m_Am_B+t+u)\\
&-c_{v_A}^{(1)}m_A(-2m_l^2+8m_Am_B+t+u))c_{v_A}^{(1)*}+m_A(c_{a_1}^{(1)}m_l^2m_A+c_{a_2}^{(1)}m_l^2m_A\\
&+4c_{a_1}^{(1)}m_l^2m_B+4c_{a_2}^{(1)}m_l^2m_B+4c_{a_1}^{(1)}m_A^2m_B+4c_{a_2}^{(1)}m_A^2m_B+c_{a_1}^{(1)}m_Am_B^2\\
&+c_{a_2}^{(1)}m_Am_B^2-c_{a_2}^{(1)}m_At-4c_{a_1}^{(1)}m_Bt+c_{a_A}^{(1)}m_A(2m_l^2+8m_Am_B-t-u)-c_{a_1}^{(1)}m_Au\\
&-4c_{a_2}^{(1)}m_Bu+c_{a_0}^{(1)}(4m_l^2+4m_Am_B-2(t+u)))c_{a_A}^{(1)*}-c_{v_1}^{(1)}m_l^4c_{v_1}^{(1)*}+c_{v_2}^{(1)}m_l^4c_{v_1}^{(1)*}\\
&-2c_{v_0}^{(1)}m_l^2m_Ac_{v_1}^{(1)*}+c_{v_A}^{(1)}m_l^2m_A^2c_{v_1}^{(1)*}+c_{v_1}^{(1)}m_l^2m_A^2c_{v_1}^{(1)*}+2c_{v_0}^{(1)}m_l^2m_Bc_{v_1}^{(1)*}\\
&-4c_{v_A}^{(1)}m_l^2m_Am_Bc_{v_1}^{(1)*}-8c_{v_1}^{(1)}m_l^2m_Am_Bc_{v_1}^{(1)*}+2c_{v_0}^{(1)}m_A^2m_Bc_{v_1}^{(1)*}\\
&-4c_{v_A}^{(1)}m_A^3m_Bc_{v_1}^{(1)*}-4c_{v_2}^{(1)}m_A^3m_Bc_{v_1}^{(1)*}+c_{v_1}^{(1)}m_l^2m_B^2c_{v_1}^{(1)*}-2c_{v_0}^{(1)}m_Am_B^2c_{v_1}^{(1)*}\\
&+c_{v_A}^{(1)}m_A^2m_B^2c_{v_1}^{(1)*}+c_{v_1}^{(1)}m_A^2m_B^2c_{v_1}^{(1)*}+c_{v_2}^{(1)}m_A^2m_B^2c_{v_1}^{(1)*}-4c_{v_2}^{(1)}m_Am_B^3c_{v_1}^{(1)*}\\
&-2c_{v_0}^{(1)}m_Btc_{v_1}^{(1)*}+4c_{v_A}^{(1)}m_Am_Btc_{v_1}^{(1)*}+4c_{v_2}^{(1)}m_Am_Btc_{v_1}^{(1)*}-c_{v_1}^{(1)}m_B^2tc_{v_1}^{(1)*}\\
&+2c_{v_0}^{(1)}m_Auc_{v_1}^{(1)*}-c_{v_A}^{(1)}m_A^2uc_{v_1}^{(1)*}-c_{v_1}^{(1)}m_A^2uc_{v_1}^{(1)*}+4c_{v_2}^{(1)}m_Am_Buc_{v_1}^{(1)*}\\
&+c_{v_1}^{(1)}tuc_{v_1}^{(1)*}-c_{v_2}^{(1)}tuc_{v_1}^{(1)*}-c_{a_1}^{(1)}m_l^4c_{a_1}^{(1)*}+c_{a_2}^{(1)}m_l^4c_{a_1}^{(1)*}+2c_{a_0}^{(1)}m_l^2m_Ac_{a_1}^{(1)*}\\
&+c_{a_A}^{(1)}m_l^2m_A^2c_{a_1}^{(1)*}+c_{a_1}^{(1)}m_l^2m_A^2c_{a_1}^{(1)*}+2c_{a_0}^{(1)}m_l^2m_Bc_{a_1}^{(1)*}+4c_{a_A}^{(1)}m_l^2m_Am_Bc_{a_1}^{(1)*}\\
&+8c_{a_1}^{(1)}m_l^2m_Am_Bc_{a_1}^{(1)*}+2c_{a_0}^{(1)}m_A^2m_Bc_{a_1}^{(1)*}+4c_{a_A}^{(1)}m_A^3m_Bc_{a_1}^{(1)*}+4c_{a_2}^{(1)}m_A^3m_Bc_{a_1}^{(1)*}
\end{aligned}$$

$$
\begin{aligned}
&+ c^{(1)}_{a_1} m_l^2 m_B^2 c^{(1)*}_{a_1} + 2c^{(1)}_{a_0} m_A m_B^2 c^{(1)*}_{a_1} + c^{(1)}_{a_A} m_A^2 m_B^2 c^{(1)*}_{a_1} + c^{(1)}_{a_1} m_A^2 m_B^2 c^{(1)*}_{a_1} \\
&+ c^{(1)}_{a_2} m_A^2 m_B^2 c^{(1)*}_{a_1} + 4c^{(1)}_{a_2} m_A m_B^3 c^{(1)*}_{a_1} - 2c^{(1)}_{a_0} m_B t c^{(1)*}_{a_1} - 4c^{(1)}_{a_A} m_A m_B t c^{(1)*}_{a_1} \\
&- 4c^{(1)}_{a_2} m_A m_B t c^{(1)*}_{a_1} - c^{(1)}_{a_1} m_B^2 t c^{(1)*}_{a_1} - 2c^{(1)}_{a_0} m_A u c^{(1)*}_{a_1} - c^{(1)}_{a_A} m_A^2 u c^{(1)*}_{a_1} \\
&- c^{(1)}_{a_1} m_A^2 u c^{(1)*}_{a_1} - 4c^{(1)}_{a_2} m_A m_B u c^{(1)*}_{a_1} + c^{(1)}_{a_1} t u c^{(1)*}_{a_1} - c^{(1)}_{a_2} t u c^{(1)*}_{a_1} \\
&+ c^{(1)}_{v_1} m_l^4 c^{(1)*}_{v_2} - c^{(1)}_{v_2} m_l^4 c^{(1)*}_{v_2} - 2c^{(1)}_{v_0} m_l^2 m_A c^{(1)*}_{v_2} + c^{(1)}_{v_A} m_l^2 m_A^2 c^{(1)*}_{v_2} \\
&+ c^{(1)}_{v_2} m_l^2 m_A^2 c^{(1)*}_{v_2} + 2c^{(1)}_{v_0} m_l^2 m_B c^{(1)*}_{v_2} - 4c^{(1)}_{v_A} m_l^2 m_A m_B c^{(1)*}_{v_2} - 8c^{(1)}_{v_2} m_l^2 m_A m_B c^{(1)*}_{v_2} \\
&+ 2c^{(1)}_{v_0} m_A^2 m_B c^{(1)*}_{v_2} - 4c^{(1)}_{v_A} m_A^3 m_B c^{(1)*}_{v_2} - 4c^{(1)}_{v_1} m_A^3 m_B c^{(1)*}_{v_2} + c^{(1)}_{v_2} m_l^2 m_B^2 c^{(1)*}_{v_2} \\
&- 2c^{(1)}_{v_0} m_A m_B^2 c^{(1)*}_{v_2} + c^{(1)}_{v_A} m_A^2 m_B^2 c^{(1)*}_{v_2} + c^{(1)}_{v_1} m_A^2 m_B^2 c^{(1)*}_{v_2} + c^{(1)}_{v_2} m_A^2 m_B^2 c^{(1)*}_{v_2} \\
&- 4c^{(1)}_{v_1} m_A m_B^3 c^{(1)*}_{v_2} + 2c^{(1)}_{v_0} m_A t c^{(1)*}_{v_2} - c^{(1)}_{v_A} m_A^2 t c^{(1)*}_{v_2} - c^{(1)}_{v_2} m_A^2 t c^{(1)*}_{v_2} \\
&+ 4c^{(1)}_{v_1} m_A m_B t c^{(1)*}_{v_2} - c^{(1)}_{v_1} t u c^{(1)*}_{v_2} - c^{(1)}_{v_2} m_B^2 u c^{(1)*}_{v_2} + c^{(1)}_{a_A} m_l^2 m_A^2 c^{(1)*}_{a_2} \\
&- 2c^{(1)}_{v_0} m_B u c^{(1)*}_{v_2} + 4c^{(1)}_{v_A} m_A m_B u c^{(1)*}_{v_2} + 4c^{(1)}_{v_1} m_A m_B u c^{(1)*}_{v_2} \\
&+ c^{(1)}_{v_2} t u c^{(1)*}_{v_2} + c^{(1)}_{a_1} m_l^4 c^{(1)*}_{a_2} - c^{(1)}_{a_2} m_l^4 c^{(1)*}_{a_2} + 2c^{(1)}_{a_0} m_l^2 m_A c^{(1)*}_{a_2} \\
&+ c^{(1)}_{a_2} m_l^2 m_A^2 c^{(1)*}_{a_2} + 2c^{(1)}_{a_0} m_l^2 m_B c^{(1)*}_{a_2} + 4c^{(1)}_{a_A} m_l^2 m_A m_B c^{(1)*}_{a_2} + 8c^{(1)}_{a_2} m_l^2 m_A m_B c^{(1)*}_{a_2} \\
&+ 2c^{(1)}_{a_0} m_A^2 m_B c^{(1)*}_{a_2} + 4c^{(1)}_{a_A} m_A^3 m_B c^{(1)*}_{a_2} + 4c^{(1)}_{a_1} m_A^3 m_B c^{(1)*}_{a_2} + c^{(1)}_{a_2} m_l^2 m_B^2 c^{(1)*}_{a_2} \\
&+ 2c^{(1)}_{a_0} m_A m_B^2 c^{(1)*}_{a_2} + c^{(1)}_{a_A} m_A^2 m_B^2 c^{(1)*}_{a_2} + c^{(1)}_{a_1} m_A^2 m_B^2 c^{(1)*}_{a_2} + c^{(1)}_{a_2} m_A^2 m_B^2 c^{(1)*}_{a_2} \\
&+ 4c^{(1)}_{a_1} m_A m_B^3 c^{(1)*}_{a_2} - 2c^{(1)}_{a_0} m_A t c^{(1)*}_{a_2} - c^{(1)}_{a_A} m_A^2 t c^{(1)*}_{a_2} - c^{(1)}_{a_2} m_A^2 t c^{(1)*}_{a_2} \\
&- 4c^{(1)}_{a_1} m_A m_B t c^{(1)*}_{a_2} - 2c^{(1)}_{a_0} m_B u c^{(1)*}_{a_2} - 4c^{(1)}_{a_A} m_A m_B u c^{(1)*}_{a_2} - 4c^{(1)}_{a_1} m_A m_B u c^{(1)*}_{a_2} \\
&- c^{(1)}_{a_2} m_B^2 u c^{(1)*}_{a_2} - c^{(1)}_{a_1} t u c^{(1)*}_{a_2} + c^{(1)}_{a_2} t u c^{(1)*}_{a_2} + 2c^{(1)}_{v_0} m_l^2 c^{(1)*}_{v_0} \\
&- 4c^{(1)}_{v_A} m_l^2 m_A c^{(1)*}_{v_0} - 2c^{(1)}_{v_1} m_l^2 m_A c^{(1)*}_{v_0} - 2c^{(1)}_{v_2} m_l^2 m_A c^{(1)*}_{v_0} + 2c^{(1)}_{v_1} m_l^2 m_B c^{(1)*}_{v_0} \\
&+ 2c^{(1)}_{v_2} m_l^2 m_B c^{(1)*}_{v_0} - 8c^{(1)}_{v_0} m_A m_B c^{(1)*}_{v_0} + 4c^{(1)}_{v_A} m_A^2 m_B c^{(1)*}_{v_0} + 2c^{(1)}_{v_1} m_A^2 m_B c^{(1)*}_{v_0} \\
&+ 2c^{(1)}_{v_2} m_A^2 m_B c^{(1)*}_{v_0} - 2c^{(1)}_{v_1} m_A m_B^2 c^{(1)*}_{v_0} - 2c^{(1)}_{v_2} m_A m_B^2 c^{(1)*}_{v_0} - c^{(1)}_{v_0} t c^{(1)*}_{v_0} \\
&+ 2c^{(1)}_{v_A} m_A t c^{(1)*}_{v_0} + 2c^{(1)}_{v_2} m_A t c^{(1)*}_{v_0} - 2c^{(1)}_{v_1} m_B t c^{(1)*}_{v_0} - c^{(1)}_{v_0} u c^{(1)*}_{v_0} \\
&+ 2c^{(1)}_{v_A} m_A u c^{(1)*}_{v_0} + 2c^{(1)}_{v_1} m_A u c^{(1)*}_{v_0} - 2c^{(1)}_{v_2} m_B u c^{(1)*}_{v_0} + 2c^{(1)}_{a_0} m_l^2 c^{(1)*}_{a_0} \\
&+ 4c^{(1)}_{a_A} m_l^2 m_A c^{(1)*}_{a_0} + 2c^{(1)}_{a_1} m_l^2 m_A c^{(1)*}_{a_0} + 2c^{(1)}_{a_2} m_l^2 m_A c^{(1)*}_{a_0} + 2c^{(1)}_{a_1} m_l^2 m_B c^{(1)*}_{a_0} \\
&+ 2c^{(1)}_{a_2} m_l^2 m_B c^{(1)*}_{a_0} + 8c^{(1)}_{a_0} m_A m_B c^{(1)*}_{a_0} + 4c^{(1)}_{a_A} m_A^2 m_B c^{(1)*}_{a_0} + 2c^{(1)}_{a_1} m_A^2 m_B c^{(1)*}_{a_0} \\
&+ 2c^{(1)}_{a_2} m_A^2 m_B c^{(1)*}_{a_0} + 2c^{(1)}_{a_1} m_A m_B^2 c^{(1)*}_{a_0} + 2c^{(1)}_{a_2} m_A m_B^2 c^{(1)*}_{a_0} - c^{(1)}_{a_0} t c^{(1)*}_{a_0} \\
&- 2c^{(1)}_{a_A} m_A t c^{(1)*}_{a_0} - 2c^{(1)}_{a_2} m_A t c^{(1)*}_{a_0} - 2c^{(1)}_{a_1} m_B t c^{(1)*}_{a_0} - c^{(1)}_{a_0} u c^{(1)*}_{a_0} \\
&- 2c^{(1)}_{a_A} m_A u c^{(1)*}_{a_0} - 2c^{(1)}_{a_1} m_A u c^{(1)*}_{a_0} - 2c^{(1)}_{a_2} m_B u c^{(1)*}_{a_0}).
\end{aligned}
\tag{C.24}
$$

Meanwhile, the interference can be written as follows

$$
\begin{aligned}
&\mathrm{Re}(\mathcal{M}_1\mathcal{M}_2^{\dagger}) = 128\mathrm{G}^4(\mathrm{m}_\mathrm{A}^2+\mathrm{m}_\mathrm{B}^2-\mathrm{t}-\mathrm{u})(\mathrm{m}_\mathrm{A}(\mathrm{c}_{\mathrm{v}_1}^{(1)}\mathrm{m}_\mathrm{l}^2\mathrm{m}_\mathrm{A}+\mathrm{c}_{\mathrm{v}_2}^{(1)}\mathrm{m}_\mathrm{l}^2\mathrm{m}_\mathrm{A}\\
&-4c_{v_1}^{(1)}m_l^2m_B-4c_{v_2}^{(1)}m_l^2m_B-4c_{v_1}^{(1)}m_A^2m_B-4c_{v_2}^{(1)}m_A^2m_B+c_{v_1}^{(1)}m_Am_B^2\\
&+c_{v_2}^{(1)}m_Am_B^2-c_{v_2}^{(1)}m_At+4c_{v_1}^{(1)}m_Bt-c_{v_1}^{(1)}m_Au+4c_{v_2}^{(1)}m_Bu\\
&+2c_{v_0}^{(1)}(-2m_l^2+2m_Am_B+t+u)-c_{v_A}^{(1)}m_A(-2m_l^2+8m_Am_B+t+u))c_{v_A}^{(2)*}\\
&+m_A(c_{a_1}^{(1)}m_l^2m_A+c_{a_2}^{(1)}m_l^2m_A+4c_{a_1}^{(1)}m_l^2m_B+4c_{a_2}^{(1)}m_l^2m_B+4c_{a_1}^{(1)}m_A^2m_B\\
&+4c_{a_2}^{(1)}m_A^2m_B+c_{a_1}^{(1)}m_Am_B^2+c_{a_2}^{(1)}m_Am_B^2-c_{a_2}^{(1)}m_At-4c_{a_1}^{(1)}m_Bt\\
&+c_{a_A}^{(1)}m_A(2m_l^2+8m_Am_B-t-u)-c_{a_1}^{(1)}m_Au-4c_{a_2}^{(1)}m_Bu\\
&+c_{a_0}^{(1)}(4m_l^2+4m_Am_B-2(t+u)))c_{a_A}^{(2)*}+c_{v_1}^{(1)}m_l^4c_{v_1}^{(2)*}-c_{v_2}^{(1)}m_l^4c_{v_1}^{(2)*}\\
&-2c_{v_0}^{(1)}m_l^2m_Ac_{v_1}^{(2)*}+c_{v_A}^{(1)}m_l^2m_A^2c_{v_1}^{(2)*}+c_{v_2}^{(1)}m_l^2m_A^2c_{v_1}^{(2)*}+2c_{v_0}^{(1)}m_l^2m_Bc_{v_1}^{(2)*}\\
&-4c_{v_A}^{(1)}m_l^2m_Am_Bc_{v_1}^{(2)*}-8c_{v_2}^{(1)}m_l^2m_Am_Bc_{v_1}^{(2)*}+2c_{v_0}^{(1)}m_A^2m_Bc_{v_1}^{(2)*}-4c_{v_A}^{(1)}m_A^3m_Bc_{v_1}^{(2)*}\\
&-4c_{v_1}^{(1)}m_A^3m_Bc_{v_1}^{(2)*}+c_{v_2}^{(1)}m_l^2m_B^2c_{v_1}^{(2)*}-2c_{v_0}^{(1)}m_Am_B^2c_{v_1}^{(2)*}+c_{v_A}^{(1)}m_A^2m_B^2c_{v_1}^{(2)*}\\
&+c_{v_1}^{(1)}m_A^2m_B^2c_{v_1}^{(2)*}+c_{v_2}^{(1)}m_A^2m_B^2c_{v_1}^{(2)*}-4c_{v_1}^{(1)}m_Am_B^3c_{v_1}^{(2)*}+2c_{v_0}^{(1)}m_Atc_{v_1}^{(2)*}\\
&-c_{v_A}^{(1)}m_A^2tc_{v_1}^{(2)*}-c_{v_2}^{(1)}m_A^2tc_{v_1}^{(2)*}+4c_{v_1}^{(1)}m_Am_Btc_{v_1}^{(2)*}-2c_{v_0}^{(1)}m_Buc_{v_1}^{(2)*}\\
&+4c_{v_A}^{(1)}m_Am_Buc_{v_1}^{(2)*}+4c_{v_1}^{(1)}m_Am_Buc_{v_1}^{(2)*}-c_{v_2}^{(1)}m_B^2uc_{v_1}^{(2)*}-c_{v_1}^{(1)}tuc_{v_1}^{(2)*}\\
&+c_{v_2}^{(1)}tuc_{v_1}^{(2)*}+c_{a_1}^{(1)}m_l^4c_{a_1}^{(2)*}-c_{a_2}^{(1)}m_l^4c_{a_1}^{(2)*}+2c_{a_0}^{(1)}m_l^2m_Ac_{a_1}^{(2)*}\\
&+c_{a_A}^{(1)}m_l^2m_A^2c_{a_1}^{(2)*}+c_{a_2}^{(1)}m_l^2m_A^2c_{a_1}^{(2)*}+2c_{a_0}^{(1)}m_l^2m_Bc_{a_1}^{(2)*}\\
&+4c_{a_A}^{(1)}m_l^2m_Am_Bc_{a_1}^{(2)*}+8c_{a_2}^{(1)}m_l^2m_Am_Bc_{a_1}^{(2)*}+2c_{a_0}^{(1)}m_A^2m_Bc_{a_1}^{(2)*}\\
&+4c_{a_A}^{(1)}m_A^3m_Bc_{a_1}^{(2)*}+4c_{a_1}^{(1)}m_A^3m_Bc_{a_1}^{(2)*}+c_{a_2}^{(1)}m_l^2m_B^2c_{a_1}^{(2)*}+2c_{a_0}^{(1)}m_Am_B^2c_{a_1}^{(2)*}\\
&+c_{a_A}^{(1)}m_A^2m_B^2c_{a_1}^{(2)*}+c_{a_1}^{(1)}m_A^2m_B^2c_{a_1}^{(2)*}+c_{a_2}^{(1)}m_A^2m_B^2c_{a_1}^{(2)*}+4c_{a_1}^{(1)}m_Am_B^3c_{a_1}^{(2)*}\\
&-2c_{a_0}^{(1)}m_Atc_{a_1}^{(2)*}-c_{a_A}^{(1)}m_A^2tc_{a_1}^{(2)*}-c_{a_2}^{(1)}m_A^2tc_{a_1}^{(2)*}-4c_{a_1}^{(1)}m_Am_Btc_{a_1}^{(2)*}\\
&-2c_{a_0}^{(1)}m_Buc_{a_1}^{(2)*}-4c_{a_A}^{(1)}m_Am_Buc_{a_1}^{(2)*}-4c_{a_1}^{(1)}m_Am_Buc_{a_1}^{(2)*}-c_{a_2}^{(1)}m_B^2uc_{a_1}^{(2)*}\\
&-c_{a_1}^{(1)}tuc_{a_1}^{(2)*}+c_{a_2}^{(1)}tuc_{a_1}^{(2)*}-c_{v_1}^{(1)}m_l^4c_{v_2}^{(2)*}+c_{v_2}^{(1)}m_l^4c_{v_2}^{(2)*}\\
&-2c_{v_0}^{(1)}m_l^2m_Ac_{v_2}^{(2)*}+c_{v_A}^{(1)}m_l^2m_A^2c_{v_2}^{(2)*}+c_{v_1}^{(1)}m_l^2m_A^2c_{v_2}^{(2)*}+2c_{v_0}^{(1)}m_l^2m_Bc_{v_2}^{(2)*}\\
&-4c_{v_A}^{(1)}m_l^2m_Am_Bc_{v_2}^{(2)*}-8c_{v_1}^{(1)}m_l^2m_Am_Bc_{v_2}^{(2)*}+2c_{v_0}^{(1)}m_A^2m_Bc_{v_2}^{(2)*}-4c_{v_A}^{(1)}m_A^3m_Bc_{v_2}^{(2)*}\\
&-4c_{v_2}^{(1)}m_A^3m_Bc_{v_2}^{(2)*}+c_{v_1}^{(1)}m_l^2m_B^2c_{v_2}^{(2)*}-2c_{v_0}^{(1)}m_Am_B^2c_{v_2}^{(2)*}+c_{v_A}^{(1)}m_A^2m_B^2c_{v_2}^{(2)*}\\
&+c_{v_1}^{(1)}m_A^2m_B^2c_{v_2}^{(2)*}+c_{v_2}^{(1)}m_A^2m_B^2c_{v_2}^{(2)*}-4c_{v_2}^{(1)}m_Am_B^3c_{v_2}^{(2)*}-2c_{v_0}^{(1)}m_Btc_{v_2}^{(2)*}\\
&+4c_{v_A}^{(1)}m_Am_Btc_{v_2}^{(2)*}+4c_{v_2}^{(1)}m_Am_Btc_{v_2}^{(2)*}-c_{v_1}^{(1)}m_B^2tc_{v_2}^{(2)*}+2c_{v_0}^{(1)}m_Auc_{v_2}^{(2)*}\\
&-c_{v_A}^{(1)}m_A^2uc_{v_2}^{(2)*}-c_{v_1}^{(1)}m_A^2uc_{v_2}^{(2)*}+4c_{v_2}^{(1)}m_Am_Buc_{v_2}^{(2)*}+c_{v_1}^{(1)}tuc_{v_2}^{(2)*}\\
&-c_{v_2}^{(1)}tuc_{v_2}^{(2)*}-c_{a_1}^{(1)}m_l^4c_{a_2}^{(2)*}+c_{a_2}^{(1)}m_l^4c_{a_2}^{(2)*}+2c_{a_0}^{(1)}m_l^2m_Ac_{a_2}^{(2)*}\\
&+c_{a_A}^{(1)}m_l^2m_A^2c_{a_2}^{(2)*}+c_{a_1}^{(1)}m_l^2m_A^2c_{a_2}^{(2)*}+2c_{a_0}^{(1)}m_l^2m_Bc_{a_2}^{(2)*}+4c_{a_A}^{(1)}m_l^2m_Am_Bc_{a_2}^{(2)*}\\
&+8c_{a_1}^{(1)}m_l^2m_Am_Bc_{a_2}^{(2)*}+2c_{a_0}^{(1)}m_A^2m_Bc_{a_2}^{(2)*}+4c_{a_A}^{(1)}m_A^3m_Bc_{a_2}^{(2)*}+4c_{a_2}^{(1)}m_A^3m_Bc_{a_2}^{(2)*}
\end{aligned}
$$

$$
\begin{aligned}
&+ c_{a_1}^{(1)} m_l^2 m_B^2 c_{a_2}^{(2)*} + 2c_{a_0}^{(1)} m_A m_B^2 c_{a_2}^{(2)*} + c_{a_A}^{(1)} m_A^2 m_B^2 c_{a_2}^{(2)*} + c_{a_1}^{(1)} m_A^2 m_B^2 c_{a_2}^{(2)*} \\
&+ c_{a_2}^{(1)} m_A^2 m_B^2 c_{a_2}^{(2)*} + 4c_{a_2}^{(1)} m_A m_B^3 c_{a_2}^{(2)*} - 2c_{a_0}^{(1)} m_B t c_{a_2}^{(2)*} - 4c_{a_A}^{(1)} m_A m_B t c_{a_2}^{(2)*} \\
&- 4c_{a_2}^{(1)} m_A m_B t c_{a_2}^{(2)*} - c_{a_1}^{(1)} m_B^2 t c_{a_2}^{(2)*} - 2c_{a_0}^{(1)} m_A u c_{a_2}^{(2)*} - c_{a_A}^{(1)} m_A^2 u c_{a_2}^{(2)*} \\
&- c_{a_1}^{(1)} m_A^2 u c_{a_2}^{(2)*} - 4c_{a_2}^{(1)} m_A m_B u c_{a_2}^{(2)*} + c_{a_1}^{(1)} t u c_{a_2}^{(2)*} - c_{a_2}^{(1)} t u c_{a_2}^{(2)*} \\
&+ 2c_{v_0}^{(1)} m_l^2 c_{v_0}^{(2)*} - 4c_{v_A}^{(1)} m_l^2 m_A c_{v_0}^{(2)*} - 2c_{v_1}^{(1)} m_l^2 m_A c_{v_0}^{(2)*} - 2c_{v_2}^{(1)} m_l^2 m_A c_{v_0}^{(2)*} \\
&+ 2c_{v_1}^{(1)} m_l^2 m_B c_{v_0}^{(2)*} + 2c_{v_2}^{(1)} m_l^2 m_B c_{v_0}^{(2)*} - 8c_{v_0}^{(1)} m_A m_B c_{v_0}^{(2)*} + 4c_{v_A}^{(1)} m_A^2 m_B c_{v_0}^{(2)*} \\
&+ 2c_{v_1}^{(1)} m_A^2 m_B c_{v_0}^{(2)*} + 2c_{v_2}^{(1)} m_A^2 m_B c_{v_0}^{(2)*} - 2c_{v_1}^{(1)} m_A m_B^2 c_{v_0}^{(2)*} - 2c_{v_2}^{(1)} m_A m_B^2 c_{v_0}^{(2)*} \\
&- c_{v_0}^{(1)} t c_{v_0}^{(2)*} + 2c_{v_A}^{(1)} m_A t c_{v_0}^{(2)*} + 2c_{v_2}^{(1)} m_A t c_{v_0}^{(2)*} - 2c_{v_1}^{(1)} m_B t c_{v_0}^{(2)*} \\
&- c_{v_0}^{(1)} u c_{v_0}^{(2)*} + 2c_{v_A}^{(1)} m_A u c_{v_0}^{(2)*} + 2c_{v_1}^{(1)} m_A u c_{v_0}^{(2)*} - 2c_{v_2}^{(1)} m_B u c_{v_0}^{(2)*} \\
&+ 2c_{a_0}^{(1)} m_l^2 c_{a_0}^{(2)*} + 4c_{a_A}^{(1)} m_l^2 m_A c_{a_0}^{(2)*} + 2c_{a_1}^{(1)} m_l^2 m_A c_{a_0}^{(2)*} + 2c_{a_2}^{(1)} m_l^2 m_A c_{a_0}^{(2)*} \\
&+ 2c_{a_1}^{(1)} m_l^2 m_B c_{a_0}^{(2)*} + 2c_{a_2}^{(1)} m_l^2 m_B c_{a_0}^{(2)*} + 8c_{a_0}^{(1)} m_A m_B c_{a_0}^{(2)*} + 4c_{a_A}^{(1)} m_A^2 m_B c_{a_0}^{(2)*} \\
&+ 2c_{a_1}^{(1)} m_A^2 m_B c_{a_0}^{(2)*} + 2c_{a_2}^{(1)} m_A^2 m_B c_{a_0}^{(2)*} + 2c_{a_1}^{(1)} m_A m_B^2 c_{a_0}^{(2)*} + 2c_{a_2}^{(1)} m_A m_B^2 c_{a_0}^{(2)*} \\
&- c_{a_0}^{(1)} t c_{a_0}^{(2)*} - 2c_{a_A}^{(1)} m_A t c_{a_0}^{(2)*} - 2c_{a_2}^{(1)} m_A t c_{a_0}^{(2)*} - 2c_{a_1}^{(1)} m_B t c_{a_0}^{(2)*} \\
&- c_{a_0}^{(1)} u c_{a_0}^{(2)*} - 2c_{a_A}^{(1)} m_A u c_{a_0}^{(2)*} - 2c_{a_1}^{(1)} m_A u c_{a_0}^{(2)*} - 2c_{a_2}^{(1)} m_B u c_{a_0}^{(2)*}).
\end{aligned}
\tag{C.25}
$$

C.1 Phase space integration

In order to get the decay width we need to integrate the squared amplitude of eq. (C.9) according to:

$$
\Gamma = \frac{1}{2(4\pi)^3 m_A^3} \int_{u_{min}}^{u_{max}} \int_{t^-}^{t^+} |\overline{\mathcal{M}_1}|^2. \tag{C.26}
$$

The limits on the Mandelstam variables u and t are given by:

$$
(m_B + m_l)^2 \leq u \leq (m_A - m_l)^2, \tag{C.27}
$$

and

$$
t^- \leq t \leq t^+ \ , \tag{C.28}
$$

where

$$
\begin{aligned}
t^{\pm} =& \frac{1}{2u} \left(2(m_A^2 + m_B^2 - u)u - (m_A^2 - m_l^2 - u)(u - m_B^2 + m_l^2) \right) \\
&\pm \frac{1}{2u} \left[\lambda^{1/2}(m_A^2, m_l^2, u) \lambda^{1/2}(u, m_B^2, m_l^2) \right]
\end{aligned}
\ . \tag{C.29}
$$

In eq(C.29), λ is defined as the Kallen function: $\lambda(x, y, z) = x^2 + y^2 + z^2 - 2(xy + xz + yz)$.

Bibliography

[1] Georges Aad et al. Observation of a new particle in the search for the Standard Model Higgs boson with the ATLAS detector at the LHC. *Phys. Lett. B*, 716:1–29, 2012.

[2] Serguei Chatrchyan et al. Observation of a New Boson at a Mass of 125 GeV with the CMS Experiment at the LHC. *Phys. Lett. B*, 716:30–61, 2012.

[3] S. L. Glashow. Partial Symmetries of Weak Interactions. *Nucl. Phys.*, 22:579–588, 1961.

[4] Steven Weinberg. A Model of Leptons. *Phys. Rev. Lett.*, 19:1264–1266, 1967.

[5] Abdus Salam. Weak and Electromagnetic Interactions. *Conf. Proc. C*, 680519:367–377, 1968.

[6] Y. Fukuda et al. Evidence for oscillation of atmospheric neutrinos. *Phys. Rev. Lett.*, 81:1562–1567, 1998.

[7] Q. R. Ahmad et al. Measurement of the rate of $\nu_e + d \rightarrow p + p + e^-$ interactions produced by ^{8}B solar neutrinos at the Sudbury Neutrino Observatory. *Phys. Rev. Lett.*, 87:071301, 2001.

[8] Felix Schlumpf. Beta decay of hyperons in a relativistic quark model. *Phys. Rev. D*, 51:2262–2270, 1995.

[9] Augusto García and Piotr Kielanowski. *The beta decay of hyperons*. 1985.

[10] Hai-Bo Li. Prospects for rare and forbidden hyperon decays at BESIII. *Front. Phys. (Beijing)*, 12(5):121301, 2017. [Erratum: Front.Phys.(Beijing) 14, 64001 (2019)].

[11] Medina Ablikim et al. Search for the lepton number violating decay $\Sigma^- \to pe^-e^-$ and the rare inclusive decay $\Sigma^- \to \Sigma^+X$. *Phys. Rev. D*, 103(5):052011, 2021.

[12] C. Barbero, G. Lopez Castro, and A. Mariano. Double beta decay of Σ^- hyperons. *Phys. Lett. B*, 566:98–107, 2003.

[13] C. Barbero, Ling-Fong Li, G. López Castro, and A. Mariano. Matrix elements of four-quark operators and $\Delta L = 2$ hyperon decays. *Phys. Rev. D*, 87(3):036010, 2013.

[14] R. N. Mohapatra et al. Theory of neutrinos: A White paper. *Rept. Prog. Phys.*, 70:1757–1867, 2007.

[15] Alessandro Strumia and Francesco Vissani. Neutrino masses and mixings and... 6 2006.

[16] S. T. Petcov. The Nature of Massive Neutrinos. *Adv. High Energy Phys.*, 2013:852987, 2013.

[17] Palash B. Pal. Dirac, Majorana and Weyl fermions. *Am. J. Phys.*, 79:485–498, 2011.

[18] Ziro Maki, Masami Nakagawa, and Shoichi Sakata. Remarks on the unified model of elementary particles. *Prog. Theor. Phys.*, 28:870–880, 1962.

[19] P. A. Zyla et al. Review of Particle Physics. *PTEP*, 2020(8):083C01, 2020.

[20] B. Pontecorvo. Neutrino Experiments and the Problem of Conservation of Leptonic Charge. *Zh. Eksp. Teor. Fiz.*, 53:1717–1725, 1967.

[21] L. Wolfenstein. Neutrino Oscillations in Matter. *Phys. Rev. D*, 17:2369–2374, 1978.

[22] R. N. Mohapatra and P. B. Pal. *Massive neutrinos in physics and astrophysics. Second edition*, volume 60. 1998.

[23] W. Grimus and L. Lavoura. The Seesaw mechanism at arbitrary order: Disentangling the small scale from the large scale. *JHEP*, 11:042, 2000.

[24] J. Schechter and J. W. F. Valle. Neutrino Masses in SU(2) x U(1) Theories. *Phys. Rev. D*, 22:2227, 1980.

[25] Srubabati Goswami, K. N. Vishnudath, and Najimuddin Khan. Constraining the minimal type-III seesaw model with naturalness, lepton flavor violation, and electroweak vacuum stability. *Phys. Rev. D*, 99(7):075012, 2019.

[26] A. Giuliani, J. J. Gomez Cadenas, S. Pascoli, E. Previtali, R. Saakyan, K. Schäffner, and S. Schönert. Double Beta Decay APPEC Committee Report. 10 2019.

[27] M. Doi, T. Kotani, and E. Takasugi. Double beta Decay and Majorana Neutrino. *Prog. Theor. Phys. Suppl.*, 83:1, 1985.

[28] W. H. Furry. On transition probabilities in double beta-disintegration. *Phys. Rev.*, 56:1184–1193, 1939.

[29] Michelle J. Dolinski, Alan W. P. Poon, and Werner Rodejohann. Neutrinoless Double-Beta Decay: Status and Prospects. *Ann. Rev. Nucl. Part. Sci.*, 69:219–251, 2019.

[30] S. M. Bilenky and C. Giunti. Neutrinoless Double-Beta Decay: a Probe of Physics Beyond the Standard Model. *Int. J. Mod. Phys. A*, 30(04n05):1530001, 2015.

[31] J. Schechter and J. W. F. Valle. Neutrinoless Double beta Decay in SU(2)xU(1) Theories. *Phys. Rev. D*, 25:2951, 1982.

[32] Rabindra N. Mohapatra and J. D. Vergados. A New Contribution to Neutrinoless Double Beta Decay in Gauge Models. *Phys. Rev. Lett.*, 47:1713–1716, 1981.

[33] G. B. Gelmini and M. Roncadelli. Left-Handed Neutrino Mass Scale and Spontaneously Broken Lepton Number. *Phys. Lett. B*, 99:411–415, 1981.

[34] J. D. Vergados. Pion double charge exchange contribution to neutrinoless double beta decay. *Phys. Rev. D*, 25:914, 1982.

[35] J. J. Gomez-Cadenas, J. Martin-Albo, M. Mezzetto, F. Monrabal, and M. Sorel. The Search for neutrinoless double beta decay. *Riv. Nuovo Cim.*, 35(2):29–98, 2012.

[36] C. Barbero, Ling-Fong Li, G. Lopez Castro, and A. Mariano. $\Delta L = 2$ hyperon semileptonic decays. *Phys. Rev. D*, 76:116008, 2007.

[37] Nicola Cabibbo, Earl C. Swallow, and Roland Winston. Semileptonic hyperon decays. *Ann. Rev. Nucl. Part. Sci.*, 53:39–75, 2003.

[38] Ansgar Denner, Stefan Dittmaier, and Lars Hofer. COLLIER - A fortran-library for one-loop integrals. *PoS*, LL2014:071, 2014.

[39] D. Rein and L. M. Sehgal. Long Distance Contributions to the Decay $K^+ \to \pi^+ \nu\bar{\nu}$. *Phys. Rev. D*, 39:3325, 1989.

[40] G. Peter Lepage and Stanley J. Brodsky. Exclusive Processes in Perturbative Quantum Chromodynamics. *Phys. Rev. D*, 22:2157, 1980.

[41] G. Hernández-Tomé, J. I. Illana, M. Masip, G. López Castro, and P. Roig. Effects of heavy Majorana neutrinos on lepton flavor violating processes. *Phys. Rev. D*, 101(7):075020, 2020.

[42] Arindam Das, Yu Gao, and Teruki Kamon. Heavy neutrino search via semileptonic Higgs decay at the LHC. *Eur. Phys. J. C*, 79(5):424, 2019.

[43] Patrick D. Bolton, Frank F. Deppisch, and P. S. Bhupal Dev. Neutrinoless double beta decay versus other probes of heavy sterile neutrinos. *JHEP*, 03:170, 2020.

[44] Enrique Fernandez-Martinez, Josu Hernandez-Garcia, and Jacobo Lopez-Pavon. Global constraints on heavy neutrino mixing. *JHEP*, 08:033, 2016.

[45] Antonio M. Coutinho, Andreas Crivellin, and Claudio Andrea Manzari. Global Fit to Modified Neutrino Couplings and the Cabibbo-Angle Anomaly. *Phys. Rev. Lett.*, 125.

[46] Ansgar Denner, H. Eck, O. Hahn, and J. Kublbeck. Feynman rules for fermion number violating interactions. *Nucl. Phys. B*, 387:467–481, 1992.

[47] Jorge C Romao. Modern techniques for one-loop calculations. *Version*, 1:263, 2004.

[48] Franz Gross. *Relativistic quantum mechanics and field theory.* John Wiley & Sons, 2008.

[49] G. Passarino and M. J. G. Veltman. One Loop Corrections for e^+e^- Annihilation Into $\mu^+\mu^-$ in the Weinberg Model. *Nucl. Phys. B*, 160:151–207, 1979.

[50] R. Mertig, M. Bohm, and Ansgar Denner. FEYN CALC: Computer algebraic calculation of Feynman amplitudes. *Comput. Phys. Commun.*, 64:345–359, 1991.

[51] Vladyslav Shtabovenko, Rolf Mertig, and Frederik Orellana. New Developments in FeynCalc 9.0. *Comput. Phys. Commun.*, 207:432–444, 2016.

[52] Vladyslav Shtabovenko, Rolf Mertig, and Frederik Orellana. FeynCalc 9.3: New features and improvements. *Comput. Phys. Commun.*, 256:107478, 2020.